

## **Developing Oncology Drugs Using Virtual Patients of Vascular Tumor Diseases**

Zvia Agur,<sup>1,2</sup> Naamah Bloch,<sup>2</sup> Boris Gorelik,<sup>2</sup> Marina Kleiman,<sup>2</sup> Yuri Kogan,<sup>1</sup> Yael Sagi,<sup>2</sup> D. Sidransky,<sup>3</sup> Yael Ronen<sup>2</sup>

<sup>1</sup>*Institute for Medical Biomathematics (IMBM), Hate'ena St., Bene-Ataroth,, Israel;*

<sup>2</sup>*Optimata Ltd., Abba Hillel St., no. 7, Ramat-Gan , Israel;* <sup>3</sup> *The Johns Hopkins University School of Medicine 600 N. Wolfe Street, Baltimore, MD, USA*

### **Contributors information:**

<sup>1</sup>*Institute for Medical Biomathematics (IMBM)*

*PO Box 282, 10 Hate'ena St., Bene-Ataroth 60991, Israel.*

*Phone: 972-3-9733075; Fax: 972-3-9733410;*

*E-mail: [agur@imbm.org](mailto:agur@imbm.org)*

<sup>2</sup>*Optimata Ltd.,*

*Abba Hillel St., no. 7*

*Ramat-Gan 52522 , Israel;*

*Phone: 972-3-7519226; Fax: 972-37519229;*

*E-mail: [agurz@optimata.com](mailto:agurz@optimata.com)*

<sup>3</sup> *The Johns Hopkins University School of Medicine*

*600 N. Wolfe Street,*

*Baltimore, MD, USA*

## Table of Contents:

<b>1. INTRODUCTION.....</b>	<b>3</b>
<b>2. MODELING ANGIOGENESIS .....</b>	<b>6</b>
2.1. Introduction.....	6
2.2. Simple two-dimensional modeling .....	7
2.3. Higher complexity models.....	10
<b>3. USE OF RIGOROUS MATHEMATICAL ANALYSIS FOR GAINING INSIGHT ON DRUG DEVELOPMENT .....</b>	<b>16</b>
3.1. Methods.....	19
3.2. Theoretical analysis of the angiogenesis model.....	22
3.3. Discussion of mathematical analysis methods.....	27
<b>4. USE OF ANGIOGENESIS MODELS IN THERANOSTICS.....</b>	<b>29</b>
4.1. Integrating <i>in silico</i> and <i>in vivo</i> models for treatment personalization.....	30
4.2. <i>In-silico</i> model suggests angiogenesis rate determines the optimal inter- dose interval of cytotoxic therapy.....	31
4.3. Factors that determine the optimal inter-dosing interval .....	32
4.4. Clinical relevance of the <i>in-silico</i> predictions .....	36
<b>5. USE OF ANGIOGENESIS MODELS IN DRUG SALVAGE: THE VIRTUAL PATIENT TECHNOLOGY .....</b>	<b>37</b>
5.1. Constructing the disease model .....	38
5.2. Constructing Synthetic Human Populations .....	38
5.3. Pharmacokinetics and Pharmacodynamics .....	39
5.4. Drug salvage case study – combining chemotherapeutic and antiangiogenic drugs .....	39
<b>6. SUMMARY AND CONCLUSIONS .....</b>	<b>44</b>
<b>REFERENCES.....</b>	<b>46</b>

## 1. Introduction

Despite growing capital investments of pharmaceutical companies in medical research and development, the number of new drugs brought into the market has dropped over the last decade. Moreover, the leading national and multinational regulatory agencies have become more cautious about approving new molecular entities, in the wake of the problems with Vioxx and other new drugs. ("Pharma 2020 - Which path will you take?" PriceWaterhouseCoopers, 2008). The resulting shortage in drugs may have serious consequences on industry, society and government, and a big crisis is foreseen if drug development becomes too risky and unprofitable. If the Pharmaceutical industry is to remain at the forefront of medical research and continue helping patients, it must become more innovative in reducing the development time and costs of new therapies.

Currently, the physical and toxicological properties of drug candidates are mostly studied *in vitro*, by screens to find molecules that "hit" a designated target. The most promising candidates are then selected to be tested in animals. *In silico* methods are used to design new molecules only where the structure of the target is known. The new Quantitative structure-activity relationship (QSAR) applications to drug development, employed to predict ADMET parameters, are often more complex to use and are relatively early in their development. The Pharmaceutical industry needs a faster and more predictive way of testing molecules before they go into man.

One strategy is to use "virtual R&D," i.e., R&D aided by computer simulations of the human body, to dramatically shorten the period of development of new drugs, and substantially reduce the chance of clinical failure, thus saving amortized costs across clinical development.

Indeed, Virtual Mice, Virtual Monkeys, and Virtual Patients have already been developed and pre-clinically and clinically validated for accuracy of prediction of

both drug efficacy and drug toxicity, as well as in suggesting improved drug regimens. For example, the use of virtual mice and Rhesus monkeys accurately simulated mice and individual Rhesus thrombopoiesis and responses to different thrombopoietin (TPO) regimens, and suggested an improved TPO regimen, which maintains drug efficacy but alleviates its immunogenic effects (Skomorovski et al., 2003). This Virtual Animal-suggested regimen keeps its superiority even following several years of TPO administration (Fatima et al., 2008). In another study, to be briefly discussed in this chapter, the use of virtual xenografted mice was prospectively validated to precisely replicate tumor shrinkage in mice xenografted by biopsied tumors of a Mesenchymal Chondrosarcoma (MCS) patient, treated by various combinations of biological and chemotherapy drugs. Up-scaling drug response parameters and embedding them in the Virtual MCS Patient resulted in an improved Docetaxel regimen, which was administered to the patient, relieving pancytopenia and stabilizing disease (Gorelik et al., 2008b).

In this chapter we will discuss the construction and use of the Virtual Patient technology. We will do so focusing on an important module of the Virtual Patient, namely, tumor vascularization. Recently, tumor vascularization has emerged as an especially important target in drug development. A study by Cancer Research (UK), based on 974 cancer drugs starting initial Phase I clinical trials since 1995, calculated there was an 18 percent probability that a drug would make it to commercial registration, as compared to 5 percent in 2004. The sharp improvement is due to more targeted drug development, which is based on a better knowledge of the biology of cancer. Most notably, kinase inhibitors are almost three times more likely to reach patients than other types of anti-cancer drug (Walker, 2008). Well-known examples of kinase inhibitors include trastuzumab (Herceptin) and Imatinib mesylate (Gleevec). Trastuzumab suppresses angiogenesis by both induction of anti-angiogenic factors and repression of pro-angiogenic factors and Imatinib mesylate impairs angiogenic capacity by normalization of vascularity. Understanding the dynamics of the complex angiogenesis-related processes is crucial for predicting long-term efficacy and safety of novel and more traditional drugs.

In this chapter we discuss the construction of a multi-scale mathematical model for angiogenesis, from the molecular scale through the tissue scale, at different levels of model complexity. Rigorous mathematical analysis of the angiogenesis model is presented, and its role in drug development discussed. Model validation in a treatment personalization case study is used to illustrate a new theranostic method, which in this case is based on angiogenesis modeling. Finally, we show how the angiogenesis model, embedded in the Virtual Patient technology, is used to demonstrate that an arrested drug candidate can be efficacious if applied in combination with Sunitinib Malate (Sutent).

## **2. Modeling Angiogenesis**

### **2.1. Introduction**

The first models of tumor angiogenesis appeared as early as mid 1970s (Deakin, 1976; Liotta et al., 1977; Saidel et al., 1976), following the new J. Folkman paradigm concerning the crucial role of vascularization in tumor development (Folkman, 1971). These works, driven by experimental data on tumor progression in animals, accounted for growth and movement of tumor cells and tumor-supporting blood vessels, and their mutual influence. Since the early 1990s, along with significant advances in the understanding, and detailed characterization of biological processes involved in tumor-blood vessel dynamics, a vast body of theoretical work has been developed by different researchers. Several groups have published studies that developed and explored mathematical models describing different aspects of tumor-induced angiogenesis, tumor growth and blood vessel dynamics. These works also addressed the significance of the above processes for chemotherapeutic, radiological or anti-angiogenic treatments. Naturally, these models significantly differ, both in their mathematical underpinnings, and in the biological phenomena they represent. In many reviews (e.g., (Alarcon et al., 2006 ; Araujo and McElwain, 2004; Mantzaris et al., 2004)) an effort was made to summarize and compare the different models. However, at present, no clear classification has been established. When attempting to present such a classification, one can select various criteria for comparison between the models. One type of criteria relates to the formal details of the modeling approaches, i.e., type of equations used. In contrast, one can classify the works by their applications, namely, the exact biological phenomena captured by the model or the clinically relevant questions to which the model can be applied.

Below we describe several mathematical models depicting tumor growth and angiogenesis. We will focus on the models that have been already verified by pre-clinical and clinical studies. From a mathematical point of view, the models we will discuss here neglect spatial aspects. Clearly, angiogenesis is a 3D-process, as well as tumor growth

itself. Consequently, most of the models developed in this field are taking into account the spatial dimensions of vessels and tumor growth. However, the immense complexity of the process, coupled with the intricacy of a spatial description, renders these models difficult to parameterize and thus almost impossible to investigate analytically and difficult to simulate numerically. All such models at present capture only a part of the full complex picture (Mantzaris et al., 2004). Yet, simpler models (as those discussed herein) can sufficiently account for observed tumor-vasculature dynamics and are used to explain and predict real experimental and clinical results, even though they overlook spatial aspects. Thus, using the models presented here allows incorporation of experimental data towards clinically meaningful validation and prediction. In addition, these models are both simple enough to allow efficient mathematical investigations and comprehensive enough to represent important components of the tumor angiogenesis.

## 2.2. Simple two-dimensional modeling

The first model we present here was proposed by Hahnfeldt et al. in 1999 (Hahnfeldt et al., 1999). This simple model consists of two coupled ordinary differential equations (ODEs) describing tumor mass and vascular support. For the tumor dynamics, the basic hypothesis is that the tumor mass ( $V$ ) (measured either in volume or cell units) follows the Gompertz growth law:

$$\dot{V} = -\lambda_1 \ln\left(\frac{V}{K}\right)V \quad (1)$$

This equation is accepted as a standard description of saturated tumor growth, supported by experimental evidence (Skehan, 1986; Spratt et al., 1996). Parameter  $\lambda_1$  is a constant relating the dimensionless expression  $\ln(V/K)$  to the growth rate. Parameter  $K$  is usually termed the carrying capacity of the tumor, to which the tumor mass always converges. From a practical point of view,  $K$  is a constant representing the maximal tumor burden the host could support, and when the tumor mass approaches this value, the growth rate is reduced to zero. This may be explained by a limitation on nutrient supply, as shown both experimentally (Freyer and Sutherland, 1980; Kunz-Schughart, 1999; Sutherland et al., 1971) and theoretically (Byrne, 1999; Greenspan, 1974; Landry et al., 1982; Marusić et

al., 1994) for avascular tumors in which growth was limited due to lack of diffusion of exterior nutrients.

The ability of the tumor to recruit a vascular system through angiogenic signaling has an augmenting effect on tumor carrying capacity, due to better availability of nutrients. This simple concept is considered in (Hahnfeldt et al., 1999) in order to represent the contribution of recruited blood vessels, and to describe the dynamics of vascular tumor growth and reaction to anti-angiogenic treatment. In this model,  $K$  is no longer assumed constant and its behavior is given by the second ODE in the general form:

$$\dot{K} = -\lambda_2 K + bS(V, K) - dI(V, K) - eKg(t). \quad (2)$$

Here,  $K$  is the time-dependent carrying capacity of the tumor, representing the effectiveness of the vascular support,  $\lambda_2$  represents the intrinsic spontaneous loss of vasculature, resulting in decrease in tumor support,  $S(V, K)$  and  $I(V, K)$  represent, respectively, the stimulatory and inhibitory effects produced by tumor and vasculature together,  $g(t)$  is current concentration of anti-angiogenic drug and  $b, d, e$  are rate constants. In order to further characterize the functions  $S(V, K)$  and  $I(V, K)$ , the authors refer to the experimental observation that stimulatory factors are local and short-lived, while inhibitory factors act over a longer range and time span (Hahnfeldt et al., 1999). The explicit formulations of these functions are established using the following argumentation. A diffusion-reaction equation for a stimulator or inhibitor concentration,  $n$ , is written where

$$\frac{\partial n}{\partial t} = D^2 \nabla^2 n - cn + s, \quad (3)$$

$D$  is a diffusion coefficient,  $c$  is the decay rate and  $s$  is a production rate, assumed to be equal to  $s_0$  inside the tumor and zero outside the tumor. To solve this equation, it is assumed that the tumor grows relatively slow,  $\partial n / \partial t = 0$ , and that the tumor is spherically symmetric of radius  $r_0$ . Via these assumptions, one can obtain explicit expression for the concentration  $n$  inside and outside the tumor:

$$n_{inside}(r) = \frac{s_0}{c} \left( 1 - (1 + u_0) e^{-u_0} \frac{\sinh(u)}{u} \right), \quad n_{outside}(r) = \frac{s_0}{c} (u_0 \cosh(u_0) - \sinh(u_0)) \frac{e^{-u}}{u}, \quad (4)$$



where  $u_0 = r_0 c^{1/2} / D$  and  $u = r c^{1/2} / D$ . Assumptions regarding the clearance rates can next be applied. For the inhibitor, it is assumed, that  $c \ll D^2 / r_0^2$ , leading to:

$$n_{inhibitor,inside}(r) \approx \frac{S_0}{6D^2} (3r_0^2 - r^2), \quad n_{inhibitor,outside}(r) \approx \frac{S_0 r_0^2}{3D^2 r}. \quad (5)$$

For the stimulator,  $c$  is assumed to be large and

$$n_{stimulator,inside}(r) \approx \frac{S_0}{c}, \quad n_{stimulator,outside}(r) \approx 0. \quad (6)$$

It is concluded that the overall impact of the inhibitor grows as  $r_0^2$ , i.e. as  $V^{2/3}$ , while the effect of the stimulator is independent of tumor size and vascularization. Thus, the inhibitor term is taken to be  $dV^{2/3}K$ , i.e. the rate of decay of  $K$  being defined by  $r_0^2$ . Further, for a similar reason it is argued that the ratio between inhibitor and stimulator terms in equation (2) will be approximately  $K^\alpha V^\beta$  with  $\alpha + \beta \approx 2/3$ . This relation gives the stimulation function in the form  $bV^\gamma K^\delta$ , where  $\gamma + \delta \approx 1$ . In (Hahnfeldt et al., 1999), this term is assumed to be of the form  $bV$ . Equation (2) then takes the form:

$$\dot{K} = -\lambda_2 K + bV - dV^{2/3}K - eKg(t). \quad (7)$$

The expression for the drug concentration is computed using the standard one-compartment linear PK model:

$$g(t) = \int_0^t C(\tau) e^{-k_e(t-\tau)} d\tau, \quad (8)$$

where  $C(\tau)$  is the rate of administration of the anti-angiogenic drug, and  $k_e$  is the elimination rate for this drug.

This model is applied to the control and treatment data for three angiogenesis inhibitors, mouse endostatin, mouse angiostatin and TNP-470 (see [11] for experimental details). The model was fit to the control data and to one dosage experiment for each drug.

Subsequently, it successfully predicted the experimental results using different dosages of endostatin and the combination of angiostatin and endostatin. Further, from the simulations it was found that in the absence of treatment, the ratio  $V/K$  increases asymptotically to 1 and the tumor size is limited. Simulations also suggested that the vasculature is more responsive to anti-angiogenic treatment, and that more continuous delivery of the drug may have enhanced efficacy.

In the continuation work (Sachs et al., 2001), the model was slightly modified, removing the linear decay term,  $\lambda_2 K$ , which has a small influence on the system dynamics. This model is found to have a single global attractor in the positive  $V, K$  quadrant, with the steady-state values  $V = K_0 = (b/d)^{3/2}$ , supporting the results of the simulations reported in (Hahnfeldt et al., 1999).

To summarize, the model presented above illustrates the application of mathematical theory to biological reasoning and practical clinical questions. The model's underlying assumptions are based on two major biological observations, namely that blood vessels in the tumor microenvironment support tumor growth, and that angiogenesis is stimulated by the tumor. Biological knowledge about the competition between the stimulatory and inhibitory angiogenesis factors is also translated into assumptions for this minimal mathematical model, which is constructed to capture these important postulated properties. This approach allows one to analyze the model and compare its predictions to the experimental data in order to check its validity. Furthermore, in this case, the model has a prognostic value, predicting the outcomes of applying a new monotherapy regimen and even drug combination.

### **2.3. Higher complexity models**


The models described below include additional details of tumor angiogenesis. Their first key feature is the introduction of one or more signaling molecules, which were discovered to be involved in angiogenic signaling. This progress in understanding the

biology of angiogenesis enables formalizing the known properties of these cytokines. An additional key feature is motivated by experimental results reporting more complex dynamics of the tumor-vasculature system, in particular, an oscillatory pattern in the growth of tumor size and vessel density (Gilead et al., 2004; Gilead and Neeman, 1999; Holash et al., 1999). Since the model in (Hahnfeldt et al., 1999) does not reflect these two features, more detailed models are required to incorporate the cytokine role in the signaling cascade and allow for non-monotonic and unstable behavior, even under no anti-cancer treatment.

First we describe the simplest model that incorporates the mediating role of angiogenic signaling by tumor cells. This model, explored in (Agur et al., 2004; Forys et al., 2005), consists of three ODEs describing the dynamics of three variables: tumor size,  $N$ , amount of protein involved in angiogenic signaling,  $P$ , and volume of blood vessels,  $V$ .

The tumor growth rate is assumed to depend on nutrient supply, which is proportional to vessel density, defined by  $E = V/N$ . Hence, the first equation:

$$\dot{N} = f_1(E)N. \quad (9)$$

Here, the function  $f_1$  is increasing,  $f_1(0) < 0$ ,  $\lim_{E \rightarrow \infty} f_1(E) > 0$ , i.e., the tumor will  decrease for zero vessel density and will grow with bounded rate for high vessel density.

The signaling protein is assumed to be secreted by the tumor as a result of nutrient deficiency:

$$\dot{P} = f_2(E)N - \delta P. \quad (10)$$

Here, the function  $f_2$  is decreasing,  $f_2(0) > 0$ ,  $\lim_{E \rightarrow \infty} f_2(E) = 0$ , i.e., when vessel density is large, the secretion of the pro-angiogenic protein drops, while at small vessel density each tumor cell secretes more protein. The second term accounts for first-order decay of the protein.

The size of the vessels is determined by the protein, as follows:

$$\dot{V} = f_3(P)V. \quad (11)$$

Here, the function  $f_3$  is increasing,  $f_3(0) < 0$ ,  $\lim_{E \rightarrow \infty} f_3(E) > 0$ , i.e., small amount of protein causes vessel regression, while high amounts induce growth of vasculature.

The model given by equations (9–11) is studied in (Agur et al., 2004; Forys et al., 2005) in numerical computations using sigmoid-like functions. It turns out that in contrast to the previous models, here no positive stable biologically relevant steady state exists. Note that the steady state  $N = P = E = 0$  is of no interest, since the model describes the dynamics of existing vascular tumors. It was analytically proven in this model that both the tumor and the vessel volume always grow monotonically showing no oscillations. The vessel density can either increase unlimitedly or stabilize at some level, so that the tumor and the vessels grow proportionally, thus resembling the behavior of the previous model. Since these modeled tumor and vascular dynamics fail to capture the full range of the observed real life cancer growth behavior, such as oscillations, one can consider the introduction of new assumptions that may enrich the model behavior.

In (Agur et al., 2004; Forys et al., 2005) the above model is extended by introducing time delays into the equations. Specifically, it is assumed that the current tumor growth rate and vessel formation rate depend on the prior vessel density and protein concentration some time before. Mathematically, this leads to the following system of delayed differential equations (DDE):

$$\dot{N} = f_1(E(t - \tau_1))N \quad (12)$$

$$\dot{P} = f_2(E)N - \delta P \quad (13)$$

$$\dot{V} = f_3(P(t - \tau_2))V. \quad (14)$$

Here all the functions are the same as in the system of equations (9–11),  $\tau_1$  and  $\tau_2$  are time delays, so, for example, tumor growth rate depends on vessel density some  $\tau_1$  time units

ago, rather than depending on the current vessel density. In Agur et al. (Agur et al., 2004) it is shown that this model exhibits a specific behavior, termed Hopf bifurcation, namely periodic oscillations of tumor size and vessel volume under some specific conditions. Since such behavior is observed in laboratory experiments in untreated animals (Arakelyan et al., 2003a), it can thus be concluded that the system of equations (12–14) is a minimal model able to reproduce the experimentally observed non-monotonic behavior of the angiogenic tumor.

In Bodnar and Forys (Bodnar and Forys) the models expressed in equations (9–11) and (12–14) are modified by introducing the logistic term into the equation for tumor growth. The addition of this term is justified by the observed deceleration in tumor growth and the existence of natural limit for the tumor size, even if no limitations are imposed by the vascular system. Thus, for the system of equations (9–11) the first equation now becomes

$$\dot{N} = \alpha N \left( 1 - \frac{N}{1 + f_1(E)} \right), \quad (15)$$

and for the system of equations with delay (12–14) the first equation becomes

$$\dot{N} = \alpha N \left( 1 - \frac{N}{1 + f_1(E(t - \tau_1))} \right). \quad (16)$$

where  $f_1$  is the same as in equation (9) and  $\alpha$  is the maximal tumor growth rate. The analysis in (Bodnar and Forys) shows that these two models always exhibit at least one stable steady state with  $N > 0$ , thus representing a realistic saturation in tumor growth. The model with delays also exhibits oscillatory behavior, similar to the model given by equations (12–14).

It should be noted that the simple concept of carrying capacity as used in (Hahnfeldt et al., 1999) was replaced in the models presented above by the more elaborated notion of vessel density, reflecting the relationship between the vessel volume and tumor size. In fact, the crucial factor governing tumor growth is the efficiency of the vascular support. To account for this, in (Arakelyan et al., 2005; Arakelyan et al., 2002) the notion of

effective vessel density (EVD) is introduced. It differs from the previously used vessel density in that it takes into consideration that different types of vasculature can contribute differently to nutrient supply. Following this notion, the blood vessels involved in tumor angiogenesis are divided into two groups – the immature vessels and the mature vessels. The more detailed description of the angiogenic process takes this distinction into account. The new vessels are formed by endothelial cells, which proliferate and migrate upon angiogenic signals. These new vessels are immature, being less stable and less efficient in nutrient supply. These vessels may undergo maturation by being covered by pericytes, the smooth muscle cells. This process is governed by a different type of signal - the maturation signal. Mature vessel can also undergo destabilization, due to weakening of maturation signals or appearance of anti-maturation signals. Experimental observations (Gilead et al., 2004; Gilead and Neeman, 1999; Holash et al., 1999) suggest that the dynamics of maturation and destabilization may be responsible for the non-monotonicity in tumor and vasculature growth. Following these hypotheses an additional model of five DDEs was proposed in Agur et al. (Agur et al., 2004). This model describes the growth of immature and mature vessels,  $V_1$  and  $V_2$ , respectively, as two inter-related processes. Two types of signaling proteins are considered. The first,  $P_1$  is secreted by tumor cells and assumed to stimulate immature vessels growth. Its role is equivalent to that of  $P$  in the previous models. The second protein,  $P_2$  stimulates maturation. It is also assumed to be secreted by tumor cells. This model takes the following form:

$$\dot{N} = f_1(E(t - \tau_1))N \quad (17)$$

$$\dot{P}_1 = f_2(E)N - \delta_1 P_1 \quad (18)$$

$$\dot{P}_2 = aN - \delta_2 P_2 \quad (19)$$

$$\dot{V}_1 = f_3(P_1(t - \tau_2))V_1 - f_4(P_2)V_1 + f_5(P_2(t - \tau_3))V_2. \quad (20)$$

$$\dot{V}_2 = f_4(P_2)V_1 + f_5(P_2(t - \tau_3))V_2. \quad (21)$$

Here equations (17, 18, 20) are similar to equations (12–14), except for the indices of  $P_1$  and  $V_1$  added here. The function  $f_4$ , accounting for the maturation rate, is positive and increasing. The function  $f_5$  computes mature vessels destabilization; it is positive and decreasing to zero. In addition, the computation of  $E$  is changed. Now it depends on both types of vessels,  $E = (\alpha_1 V_1 + \alpha_2 V_2)/N$ ,  $\alpha_1$  and  $\alpha_2$  being the relative contribution of

immature and mature vessels to the effective vessel density. In this work they both were taken to be 1. This model also exhibits oscillatory behavior, suggesting the possible role of blood vessels maturation and destabilization in tumor growth.

Finally, a more comprehensive model of the processes discussed above has been developed in order to better represent experiments where human ovary carcinoma spheroid were implanted in mice and tumor growth as well as immature and mature vascular dynamics were monitored *in vivo* (Arakelyan et al., 2005; Arakelyan et al., 2002). This model is formulated in terms of difference equations discrete in time and also, by ODE formalism (analyzed in the next section). The model captures the dynamics of the angiogenic tumor, calculating the following variables over time: 1) tumor size, 2) immature vessels density, 3) mature vessels density, 4) number of endothelial cells, 5) number of pericytes, 6) concentration of angiogenic factor VEGF, 7) concentration of maturation factor PDGF, 8) concentration of pro-maturation factor Angiopoietin1 (to be denoted Ang1), and 9) concentration of its competitor, anti-maturation factor Angiopoietin 2 (to be denoted Ang2). The equations for these variables reflect the biological understanding of the role of the system components, similar to the models described above. We refer the reader to Arakelyan et al. (Arakelyan et al., 2002) for more detailed description.

In Arakelyan et al. (Arakelyan et al., 2002) it is shown that, consistent with the simpler models: if the maturation process is neglected, tumor and vasculature growth become monotonic. In contrast, the introduction of vessel maturation and their destabilization dynamics into the model reduces tumor growth and leads to highly non-monotonic behavior, including irregular oscillations of tumor and vasculature size. Further, by simulating anti-VEGF and anti-PDGF treatments, it was demonstrated that anti-angiogenic treatment alone will not suffice to eliminate the tumor and has to be combined with anti-maturation treatment. This prediction has been corroborated in the pre-clinical setting by showing in pancreatic cancer mouse models that the combination of a VEGFR inhibitor with another distinctive kinase inhibitor targeting PDGFR activity (Gleevec) was able to regress late-stage tumors (Bergers et al., 2003).

In Arakelyan et al. (Arakelyan et al., 2005) this model was applied to results of animal experiments, in which implanted tumor size and vascularization were measured. The model was able to fit quantitatively the experimental data, including non-monotonic changes of tumor size and mature and immature vessel density. The model predictions of subtle behaviors of mature and immature vessel dynamics were confirmed experimentally.

In summary, a more accurate and detailed description of system dynamics can be obtained using more complex models, which account for known relevant components and processes. Even more importantly, mathematical modeling allows one to determine the minimal necessary components required to produce the observed phenomena and to understand how the complex behavior emerges from basic system properties. Once experimentally validated, the model can be used to assist researchers to improve and accelerate drug development and help identify the most prominent treatment approaches.

### **3. Use of rigorous mathematical analysis for gaining insight on drug development**

Theoretical and numerical analysis are crucial elements in the development of a mathematical model that aims to mimic any realistic behavior of a biological or physical system. It enables one to take into consideration the types of behavior patterns that the model can reproduce. Typically, one would like to examine the robustness of the model to its initial conditions and check whether chaotic, periodic or other types of behavior can arise. For example, comparing transfer function rates in dynamical systems can identify key processes thereby enhancing biological understanding. Under specific conditions analysis enables dissociation of certain parts of the model from others, and the consequences of decoupling these elements can be examined. When this occurs, one can



test whether the model can be reduced to a simpler model. Analysis of the reduced model is frequently easier and can lead to a wider understanding of the system.

At the steady state of a dynamical system, all variables remain constant. Underlying processes may still be active in the steady state, yet the ongoing processes cancel out. An example of such processes is when constant production and elimination are equal in magnitude. Mathematically, the steady state of the system is denoted a *fixed point* of a system at a point where all the time derivatives of the system vanish simultaneously. At the fixed point, the steady state problem is equivalent to solving a set of equations (in our case this set of equations is non-linear). Finding the fixed points of the system and understanding its in- and outflow, can provide knowledge on the behavior patterns of the system.

The flow problem is referred to as stability analysis. It is addressed by checking how perturbations around the fixed point evolve in time. Fixed points can be characterized in several manners. Among them are 1) *stable fixed points*, where the system tends towards the fixed point; 2) *unstable fixed points*, where the system diverges away from the fixed point; 3) *limit cycle*, where the system revolves in cycles around the fixed point.

The phase plane is a mathematical representation of the model variables at different time points and their values. The phase plane analysis reveals the various behavior patterns of the system. In order to check the stability of the whole system, the Jacobian, matrix of partial derivatives, is calculated. Often numerical simulations are performed to create a map of possible points of the system. In this map, arrows indicate flow directions between points. This information is pivotal for the comprehension of the model regardless of our ability to analyze the whole phase plane.

The types of questions we would like to answer by this stability analysis are the following: How many fixed points exist? Where in the phase plane do these fixed points occur? Are these fixed points stable? Are the identified fixed points biologically reasonable? For instance, a trivial example of an unreasonably biological fixed point is

when the system variables take negative values. These data regarding the biologically feasible steady state conditions are of great relevance. In this way, steady state analysis sheds light on how to stabilize or destabilize a biological system. This insight could be crucial in drug development efforts.

Establishing the existence of one or more fixed points in a solid tumor system, other than the obvious tumor free one, is not trivial. Clinically, there is no significant evidence of stable untreated cancer patients. The prerequisite clinical success is to eliminate the tumor, that is to achieve a complete response. However, a more likely possibility may be to transform a progressive disease into a chronic disease by stabilizing tumor progression. It is important to note that introduction of a drug to the system can give rise to additional fixed points. The existence of such additional fixed points will depend on the specific pharmacokinetic/pharmacodynamic (PK/PD) profile of that drug.

The behavior around the fixed points is important. Although, clinically, we are interested in stabilizing or reducing tumor size, model parameters other than tumor size, such as growth factors and vessel density, are of a great relevance, as they dictate the behavior of the entire tumor. Thus, mathematical analysis of these factors is instrumental for proper targeting during the drug discovery process, and can serve in the target selection and validation processes. For example, targeting angiogenesis alone, by administering anti-angiogenic monotherapy, is known to only delay tumor progression (Quesada et al., 2007). This phenomenon is an example of a system that does not converge to a fixed point (steady state) despite the imposed perturbations (pharmacotherapy). Furthermore, thresholds on variable levels may determine to which stable fixed point the system eventually converges.

In this section we attempt to find fixed points in a complex biological system for a vascular tumor (VT) model. The model underlying the work presented here was described and analyzed previously (Agur et al., 2008; Arakelyan et al., 2003b; Arakelyan et al., 2005; Arakelyan et al., 2002). The model in its simplified version is described here by a set of non-linear ordinary differential equations (ODE). We show

that this system has a non-trivial fixed point, and define the conditions for its existence. For further explanation on fixed point the reader is referred to Lee A. Segel (Segel, 1984).

### **3.1. Methods**

Here we provide an example of a mathematical analysis searching for a fixed point in a biological nonlinear system. The model at hand is an angiogenesis dependent solid tumor model. This model is a simplified version of Arakelyan et al., 2002 (Arakelyan et al., 2002). The variables that represent this simplified model may be divided into three main groups.

1. The tumor variables; the number of living tumor cells,  $L$ , and the number of necrotic tumor cells,  $N$ . Both these variables are measured in volume in units of  $\text{mm}^3$
2. The growth factors concentrations; consisting of Vascular Endothelial Growth Factor (VEGF), Platelet Derived Growth Factor (PDGF), Angiopoetin1 (Ang1) and Angiopoetin2 (Ang2); their amounts are measured in nanograms per milliliter (ng/ml)
3. The vessel related variables; consisting of volumes of immature vessels,  $V_{im}$ , mature vessels,  $V_{mat}$ , and free Perycrite cells,  $Per$ ; their amounts, are measured in  $\text{mm}^3$ . The nutrition supply to the tumor is evaluated by the Effective Vessels Density, EVD (Arakelyan et al., 2002), which is dependent on the vessel related variables and the tumor related variables.

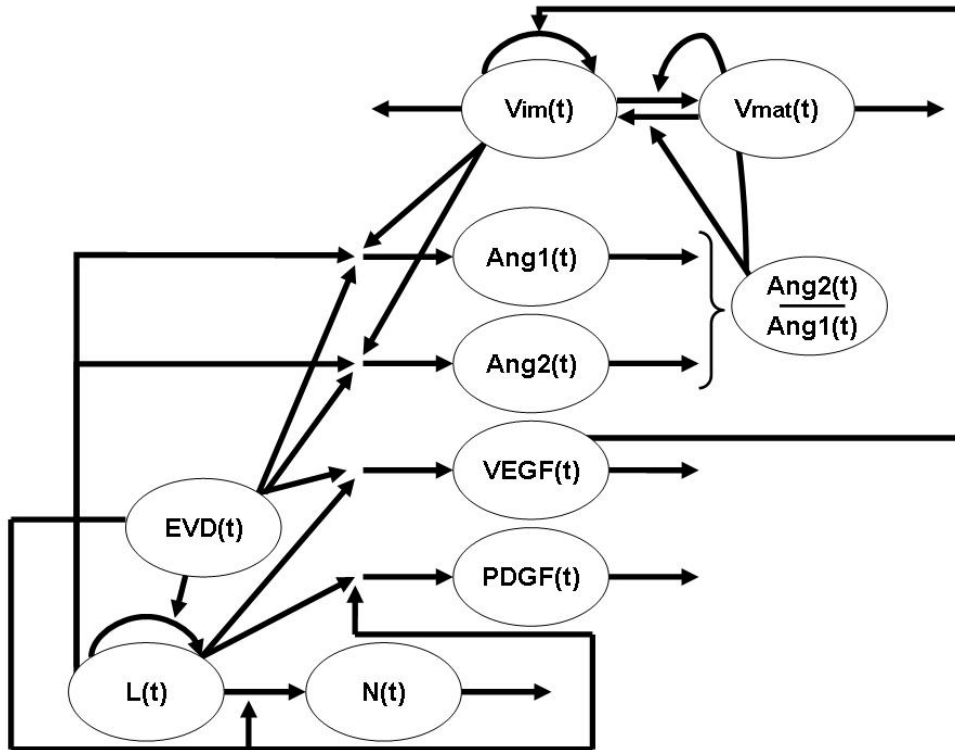


**Figure 1.** A scheme of the mathematical model for vascular tumor growth (Arakelyan et al., 2002). The notation for molecular and cellular entities is defined in the text.

The main model assumptions are listed below (see also Fig. 1).

- Living cells,  $L(t)$ , can proliferate and can undergo necrosis. Both processes are controlled by transfer function of nutrient supply to the tumor, EVD.
- The number of necrotic cells grows according to the death of the living cells controlled by EVD
- VEGF(t) is secreted by the living cells,  $L(t)$ , and its secretion is controlled by the nutrient supply to the tumor, EVD. VEGF disintegrates with a characteristic disintegration time.
- PDGF(t) is secreted by the living cells,  $L(t)$ , and its secretion is controlled by the nutrient supply to the tumor, EVD. PDGF also disintegrates.
- Ang1(t) is secreted by the living cells,  $L(t)$ . Ang1(t) is also produced by immature vessels. Its secretion in both cases is controlled by the nutrient supply to the tumor, EVD. Ang1 also disintegrates.

- $Ang2(t)$  is treated in a similar manner as  $Ang1(t)$ .
- Immature vessels may form mature vessels. This maturation process is controlled via transfer functions dependent on the amount of  $Ang1$  and by the  $Ang1$  to  $Ang2$  ratio. Destabilization of mature vessels occurs when mature vessels shed pericytes and turn again to become immature vessels. This is controlled via transfer functions dependent on the amount of  $Ang1$ ,  $Ang2$  and on the  $Ang2$  to  $Ang1$  ratio, thus enlarging the immature vessels pool. Immature vessels may also disintegrate in a characteristic time.
- Mature vessels,  $V_{mat}(t)$ , are formed when immature vessels mature. These are exactly the same Vessels that were subtracted from the immature vessels term. As mentioned above, this process is controlled via a transfer functions dependent on the amount of  $Ang1$  and on the  $Ang1$  to  $Ang2$  ratio. Destabilization of mature vessels is controlled via transfer functions dependent on the amount of  $Ang1$ ,  $Ang2$  and on the  $Ang2$  to  $Ang1$  ratio. Mature vessels can not disintegrate naturally. However we added this term to the model to allow for a later drug effect on drug related mature vessels functionality/disintegration.

To efficiently analyze the system, we utilize the fixed point definition, the point where all time derivatives vanish, to relate a single model variable to all other model variables. In addition to model variables, this mathematical expression also involves model parameter values. As an example of this approach, we consider the volume of immature vessels in the tumor,  $V_{im}$ , as the single variable. Other choices would not alter the results.

We survey the model equations to identify their inner relations at the fixed point. First, we analyze the system as a whole, checking for the existence of fixed points. Secondly, we verify the possibility that this point(s) exists within the biologically realistic parameter space (e.g., positive values of variables, such as cell numbers). We also show the existence of biologically relevant constraints on the system parameters. In this case these constrained parameters can be growth factor production rates, replication rates, etc. Finally, we suggest a numerical method for identifying clinically relevant fixed points based on the mathematical analysis.

## 3.2. Theoretical analysis of the angiogenesis model

### Fixed point analysis of the equation for living cells

The living cell equations at the fixed point is expressed as follows:

$$\dot{L} = \lambda_L \vec{f}_L(EVD)L - \mu_L \overleftarrow{f}_L(EVD)L \quad (19)$$

Here we establish the following definitions and relations:

- $\vec{f}_L(EVD)$  is a monotonically increasing transfer function bounded by two asymptotes at 0 and 1.
- $\overleftarrow{f}_L(EVD)$  is a monotonically decreasing transfer function bounded by two asymptotes at 0 and 1.
- $EVD=F(Vim, Vmat, L)$

Demanding that the derivative of the living cells numbers vanishes  $\dot{L}=0$  yields the trivial zero solution and an additional solution:

$$\rightarrow \frac{\vec{f}_L(EVD)}{\overleftarrow{f}_L(EVD)} = \frac{\lambda_L}{\mu_L} \quad (20)$$

The existence of such an EVD, as in equation (20), depends on an overlap in the effectively non-zero parts of the transfer functions. As the increasing and decreasing functions describe modification of proliferation and death as a function of nutrition supply, it is obvious that the functions overlap to some extent. Equation (20) defines a unique value, or values, for EVD which is used in the analysis for the rest of the equations.

### Necrotic cells

The death of cells is described by:

$$\dot{N} = \mu_L \overline{f}_L(EVD)L - \mu_N N \quad (21)$$

so

$$\rightarrow N_0 = \frac{\mu_L}{\mu_N} \overline{f}_L(EVD)L_0 \quad (22)$$

Substituting the expression obtained from EVD in equation (20) in  $\overline{f}_L(EVD)$  above yields a fixed point for N, the number of cells in necrosis, which depend solely on L. Hence,  $N_0$ , the number at the fixed point of necrotic cells, is related to  $L_0$ , the number of living cells, at the fixed point, and the already determined EVD value at the fixed point.

### **VEGF growth factor**

Similar to the necrotic cells case, the VEGF level fixed point,  $VEGF_0$ , is obtained as a function of the living cell fixed point and EVD

$$\dot{VEGF} = \lambda_{VEGF}^L \overline{f}_{VEGF}^L(EVD)L - \mu_{VEGF} VEGF \quad (23)$$

so

$$\rightarrow VEGF_0 = \frac{\lambda_{VEGF}^L}{\mu_{VEGF}} \overline{f}_{VEGF}^L(EVD)L_0 \quad (24)$$

The level of VEGF at the fixed point depends on the living cells and the EVD value at the fixed point.

### **PDGF growth factor**

The PDGF fixed point is dictated by the living cells, similarly to the described above. In our system, PDGF secretion influences pericyte production.

### Ang1 growth factor

The growth factors Ang1 and Ang2 are secreted by living cells and by endothelial cells that comprise the immature vessels:

$$\begin{aligned} \dot{Ang1} &= \lambda_{Ang1}^L \overline{f_{Ang1}^L} (EVD)L \\ &+ \lambda_{Ang1}^{Vim} \overline{f_{Ang1}^{Vim}} (EVD)Vim - \mu_{Ang1} Ang1 \end{aligned} \quad (25)$$

Demanding that  $\dot{Ang1} = 0$

$$\begin{aligned} Ang1_0 &= \frac{\lambda_{Ang1}^L \overline{f_{Ang1}^L} (EVD)L}{\mu_{Ang1}} \\ &+ \frac{\lambda_{Ang1}^{Vim} \overline{f_{Ang1}^{Vim}} (EVD)Vim}{\mu_{Ang1}} \end{aligned} \quad (26)$$

### Ang2 growth factor

$$\begin{aligned} \dot{Ang2} &= \lambda_{Ang2}^L \overline{f_{Ang2}^L} (EVD)L \\ &+ \lambda_{Ang2}^{Vim} \overline{f_{Ang2}^{Vim}} (EVD)Vim - \mu_{Ang2} Ang2 \end{aligned} \quad (27)$$

Demanding that  $\dot{Ang2} = 0$ , Ang2's fixed point is obtained similarly to Ang1's. The levels of Ang2 and Ang1 at the fixed point depend on the number of living cells and the density of immature vessels at the fixed point, in addition to the EVD determined by equation (20).

### Vessels fixed points



Immature vessels can proliferate. They are subtracted from the system when undergoing maturation, and they can be added to the system by mature vessels destabilization. They can also regress. The equation describing the immature vessel dynamics is therefore:

$$\begin{aligned} \dot{V}_{im} = & \lambda_{VEGF}^{V_{im}} \vec{f}_{VEGF}^{V_{im}}(VEGF)V_{im} \\ & + F(V_{mat}) \\ & - F(P, V_{im}) \\ & - \mu_{V_{mat}} \end{aligned} \quad (28)$$

The equations describing the mature vessel dynamics are governed by mature vessel creation by maturation of immature vessels and their destabilization.

$$\begin{aligned} \dot{V}_{mat} = & F(P, V_{im}) \\ & - F(V_{mat}) \\ & - \mu_{V_{mat}} \end{aligned} \quad (29)$$

Adding up these two equations, upon demanding a fixed point  $\dot{V}_{im}=0$  and  $\dot{V}_{mat}=0$ , yields a rather simple connection. Note: some model elements do not appear in the steady state solution as they have been canceled out., The following result does not depend on their specific form:

$$\lambda_{VEGF}^{V_{im}} \vec{f}_{VEGF}^{V_{im}}(VEGF)V_{im} - \mu_{V_{im}} V_{im} = \mu_{V_{mat}} V_{mat} \quad (30)$$

This equation has important consequences as detailed below.

- 1) Links between  $V_{mat}$  to  $V_{im}$  at the fixed point by substituting in equation (30), three connections that were already described;
  - Volume of living cells,  $L$ , relation to  $V_{mat}$  and  $V_{im}$  that is defined by the expression of EVD and its value at the fixed point.
  - The living cells are related to the dead cells in equation (22).
  - VEGF is related to  $L$  in equation (24).

Furthermore, once  $V_{mat_0}$  is related to  $V_{im_0}$  the expression for  $EVD_0$  can relate the living cells  $L_0$  to  $V_{im_0}$ .

- 2) Another important consequence is revealed when we consider a system that lacks mature vessels ( $V_{mat}=0$ ) (for example very early in the tumor progression when mature vessels have not been formed yet or under some medication when mature vessels can not be formed) in equation (30)

$$\lambda_{VEGF}^{V_{im}} \bar{f}_{VEGF}^{V_{im}}(VEGF) - \mu_{V_{im}} = 0 \quad (31)$$

$$\rightarrow \bar{f}_{VEGF}^{V_{im}}(VEGF) = \frac{\mu_{V_{im}}}{\lambda_{VEGF}^{V_{im}}}$$

The transfer function values  $\bar{f}_{VEGF}^{V_{im}}(VEGF)$  are limited by two horizontal asymptotes at zero and 1. Clearly, a meaningful result for equation (31) is obtained only if  $\lambda_{VEGF}^{V_{im}} > \mu_{V_{im}}$ , so that the transfer function values are smaller than 1. This gives a non-trivial biological constraint in this case ( $V_{mat}=0$ ) on the proliferation rate of the immature vessels relative to their regression rate.

It is possible to look for other fixed points where mature vessels are present in the model. This can be done only numerically, as the resulting system can be highly non linear. For these fixed points, the pericytes that cover vessels walls during the maturation process can be related to the immature vessels  $V_{im}$ . This relationship is added to the previously described connections between the rest of the variables and  $V_{im}$ . Thus, a graphical solution to the general problem can be obtained by plotting  $V_{mat}=F(V_{im})$  and finding the intersection with the abscissa. We note that in this case the existence of such a fixed point can depend on the parameter values. No additional fixed points were found for any specific selection of parameters (not shown).

### **3.3. Discussion of mathematical analysis methods**

Solid tumors are an extremely complicated biological system that involves a plethora of internal and external factors. The theoretical analysis of an angiogenesis-dependent vascular tumor model described above was able to identify a non-trivial fixed point in this complex system. We found that there is a constraint on the existence of this fixed point, namely, that it exists when the immature vessel proliferation rate exceeds its death rate. This intriguing result, which may bear important consequences for anti-angiogenic therapy, could not have been found without a mathematical examination of a formal, simplified description of the system. Biologically, the fixed point that was identified here was characterized by the absence of mature vessels from the system. This finding implies that targeting vessel maturation and destabilizing already existing mature vessels may force the tumor to a fixed point. The stability of this fixed point is yet to be determined.

Other fixed points may also exist. A complex multidimensional system, such as the one described above, is practically impossible to analyze theoretically. Hence, a numerical analysis is required. The phase plane was numerically investigated for other fixed points by plotting the time derivative of the variables representing mature vessels with respect to the variable representing the immature vessels, as described above. It is important to stress again that in contrast to our general theoretical analysis, this method is numerical and thus depends on the specific choice of parameters. No additional fixed points were found in this numerical analysis.

Numerical stability analysis was also performed. For a specific choice of parameters, calculation of the Jacobian revealed that the system was not stable, but rather had potentially stable directions. Simulating behavior that results from perturbations around the fixed point (data not shown) supported this finding.

The existence of a fixed point and its stability in such a system can have significant consequences for drug development, by supporting the “go-no go” decision in the

early stages of target validation and drug discovery. For example, such an analysis can reveal if targeting certain system components is likely to have clinically desired outcomes. It can also help identify those variables that are robust to perturbations. Moreover, one can analyze combinations of several drugs that have different mechanisms of actions in order to assess their stabilizing potentials. This analysis will help in comparing between drugs with different mechanism of actions and in predicting their degree of synergy.

#### **4. Use of angiogenesis models in theranostics**

Theranostics is a collection of diagnostic techniques that guide the choice of individually tuned therapy with the aim of finding the best possible treatment for a given patient. The human genome project (Venter et al., 2001) , Protein Structure Initiative (Matthews, 2007) and recent identification of many molecular pathways have resulted in the discovery of novel targets for treating inflammatory, infectious, neurological and oncological diseases

The relevance of theranostic approaches is higher in multifactor conditions that are characterized by a high inter-patient variability. In these cases the amount of biological knowledge and clinical experience does not allow for efficient rationalization of treatment selection and requires a systematic and rational approach. In the context of cancer, theranostic approaches include imaging techniques (for example, Radioimaging/MRI etc., (Chao, 2007; Kimura et al., 2008; Wieder et al., 2007)) and biomarker identification in the blood or at the cellular levels (for example, (Iwao-Koizumi et al., 2005; Karam et al., 2008; McLeod, 2002; Salter et al., 2008)).

#### **4.1. Integrating *in silico* and *in vivo* models for treatment personalization**

Mesenchymal Chondrosarcoma (MCS) is a rare malignant disease, with as few as 100 new diagnosed patients each year in the U.S. One such patient was diagnosed with mediastinal located MCS at age 45. Shortly after the resection of the primary tumor, multiple bilateral pulmonary nodules were discovered. The patient underwent aggressive chemotherapy that included ifosfamide, cisplatin, etoposide, vincristine, doxorubicin, cyclophosphamide, and dactinomycin and sunitinib. Despite the chemotherapy, additional liver and bone metastases appeared. In addition, the patient developed severe myelosuppression with pancytopenia.

In order to determine the best possible treatment for this MCS patient, tumor fragments were taken from his lung metastases and implanted in mice. This xenograft model was established and amplified until a sufficient tumor was available to implant in a control and several treatment groups of mice. These animals were then used to compare the different pharmacotherapy regimens. We refer to this model, in which the cells are taken from the patient and never propagated as a cell line as "tumor graft" to distinguish it from the cell line xenograft models.

A general mathematical model for angiogenesis-dependant solid tumor, which was described earlier in this chapter, was utilized to perform *in silico* experiments, identical to those performed in the tumor graft model, for predicting the MCS dynamics in the control and treated animals. Pharmacokinetics (PK)/ pharmacodynamics (PD) models of the relevant drugs were constructed using publicly available data. In addition, qualitative chemosensitivity tests of several cytotoxic drugs were performed on tumor cells from the patient's biopsy. Incorporating the data of these chemosensitivity tests into the calculations allowed a certain level of personalization of otherwise general PK/PD models.

The mathematical model of the MCS tumor grafts was successfully validated with an average accuracy of 81.6% (Ziv et al., 2006) and was later fine-tuned to provide 87.2%

accuracy (Gorelik et al., 2008a). After the validation of the mathematical model, gene expression analysis of key proteins in the grafted tumors and in the MCS patient was performed in order to adjust the model to describe the tumor dynamics in the human. The resulting mathematical model of the human disease was used to perform patient-specific predictions of various anti-cancer treatments.

Guided by the results of the personalized *in silico/in vivo* combined model, clinicians administered the MCS patient once-weekly regimen of Docetaxel (DOC) – a cytotoxic agent that is routinely given every three weeks. Eventually, the patient had a dramatic response to therapy with a marked decrease in serum alkaline phosphatase from bone and an immediate substantial recovery of all 3 blood elements (hemoglobin, white blood cells and platelet count). Soft tissue disease in the lungs and liver remained stable and the patient enjoyed a 6 month period of good quality of life, ending only after pulmonary progression of his disease to which he finally succumbed (Gorelik et al., 2008a).

#### **4.2. *In-silico* model suggests angiogenesis rate determines the optimal inter-dose interval of cytotoxic therapy**

According to the simulations with the human MCS computer model that compared the efficacy of DOC delivery every 7, 14, 21 or 28 days (keeping the same average weekly dose), once weekly regimen was found to be more efficacious than the alternatives (Fig. 2). This finding is of interest due to the controversial clinical evidence regarding the relative efficacy of once- vs. tri-weekly DOC regimens. Moreover, once weekly administration of DOC is problematic due to increased adverse effects and reduced compliance (Chen et al., 2008; Warm et al., 2007). Thus one would like to identify patients that are more likely to benefit from weekly chemotherapy schedules, compared to less frequent regimens.

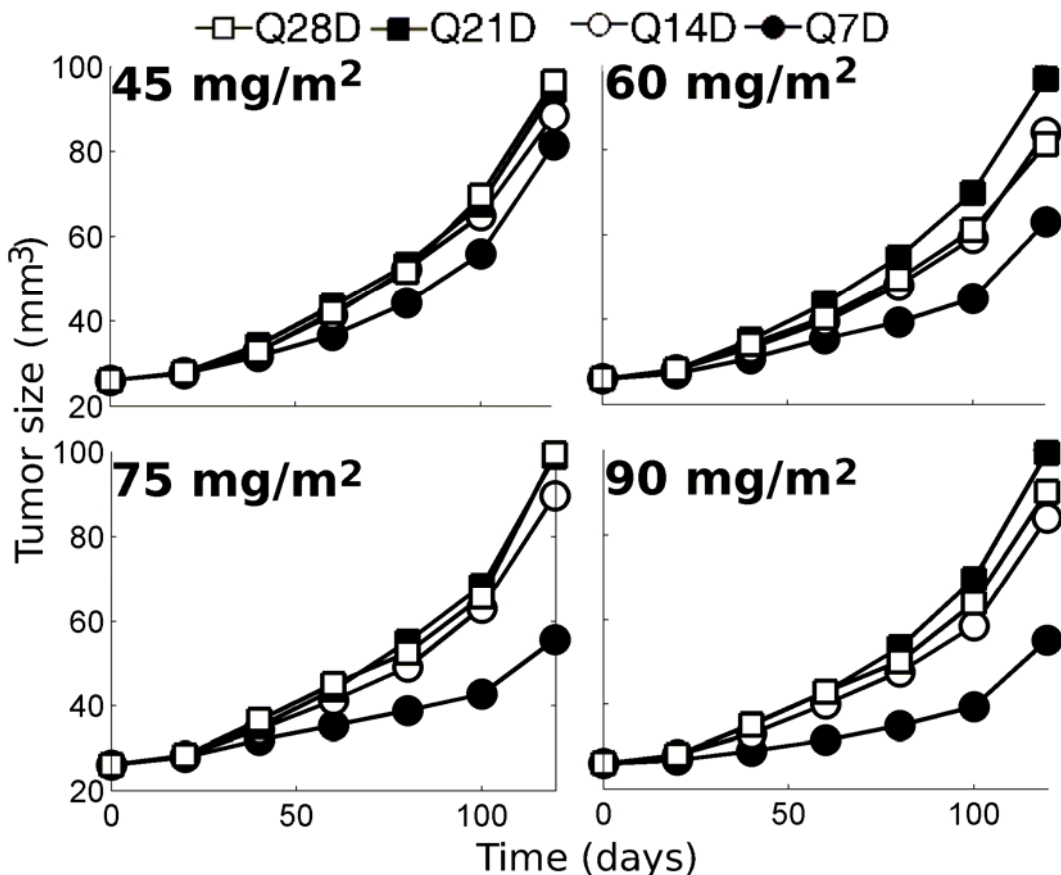


**Figure 2** Effects of DOC inter-dosing interval on tumor dynamics as predicted by simulations of the *in vivo* MCS patient's model under sixteen BEV and DOC combinations. Schedules include BEV 15mg/kg given every 21 days, combined with DOC, 1 hour IV infusion of 45 mg/m<sup>2</sup>, 60 mg/m<sup>2</sup>, 75mg/m<sup>2</sup> and 90mg/m<sup>2</sup>; four DOC administration schedules are presented: every 7, 14, 21 and 28 days (Q7D, Q14D, Q21D and Q28D, respectively).

### 4.3. Factors that determine the optimal inter-dosing interval

Maximum tumor growth rate occurs when cellular proliferation and angiogenesis work in unison (Agur, 1986, 1998; Agur et al., 2004; Agur et al., 1988, 1992). Cytotoxic agents such as, but not limited to, DOC disturb the dynamic equilibrium between the growing tumor mass and the vessel bed that support it by direct killing of tumor cells. As a consequence, a cascade of compensating events is triggered.

Tumor recovery time is a crucial factor in determining the inter-dosing interval. To illustrate this concept, consider a tumor that is exposed to a dose of a cytotoxic



compound. If the time period before the administration of the subsequent dose is not big enough for the tumor to recover to its pre-treatment size, then the net result will be tumor shrinkage. If, however, the second dose is delivered after recovery occurs, the therapy will result in a steady growth of the tumor.

To assess tumor recovery from the cytotoxic shock, let us define tumor growth inhibition (TGI) factor,  $TGI_L$ , in terms of the volume of the living cells in the tumor model before and after the treatment:

$$TGI_L (\%) = 100 \cdot \left( 1 - \frac{T_{L,t} - T_{L,0}}{C_{L,t} - C_{L,0}} \right),$$

where  $T_{L,0}$ ,  $C_{L,0}$  are initial volumes of the living cells in the treated and the control tumor, respectively;  $T_{L,t}$  and  $C_{L,t}$  are, respectively, the simulated volumes of the living cells in treated or control tumors at time  $t$ .  $TGI_L$  has a value of zero if the simulated volume of the living cells in the treated tumor equals to that in the control, untreated, tumor at the given time point. Larger  $TGI_L$  values indicate greater tumor inhibition, while negative  $TGI_L$  values indicate the situation where the simulated treated tumor is bigger (in terms of living cells volume) than the untreated one. In the clinical context, negative  $TGI_L$  values mean that the treatment was harmful rather than beneficial.

In the human MCS model simulations, the  $TGI_L$  value 7 days after a single DOC administration was 46%. As time goes on, this cytotoxic effect decreases to the value of 10% at day 21 – a difference of 36% (Fig. 3). Thus, if the second DOC dose is delivered on day 21, after substantial tumor recovery, the overall efficacy of the treatment would be smaller than the once-weekly regimens.

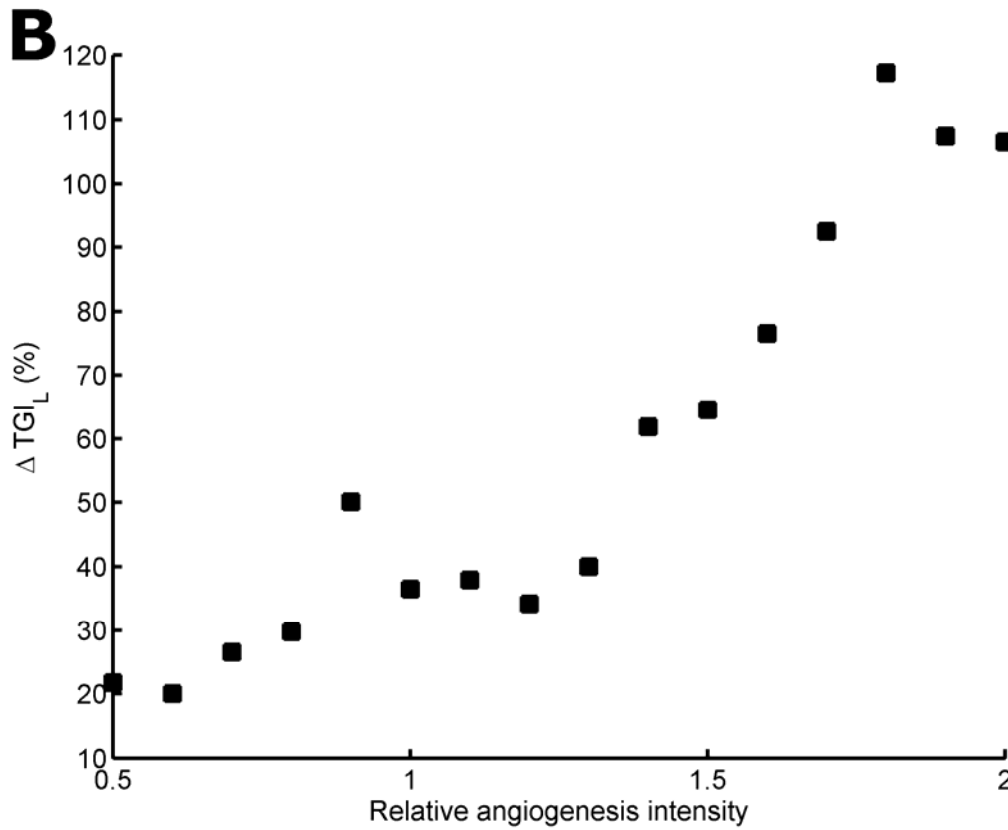
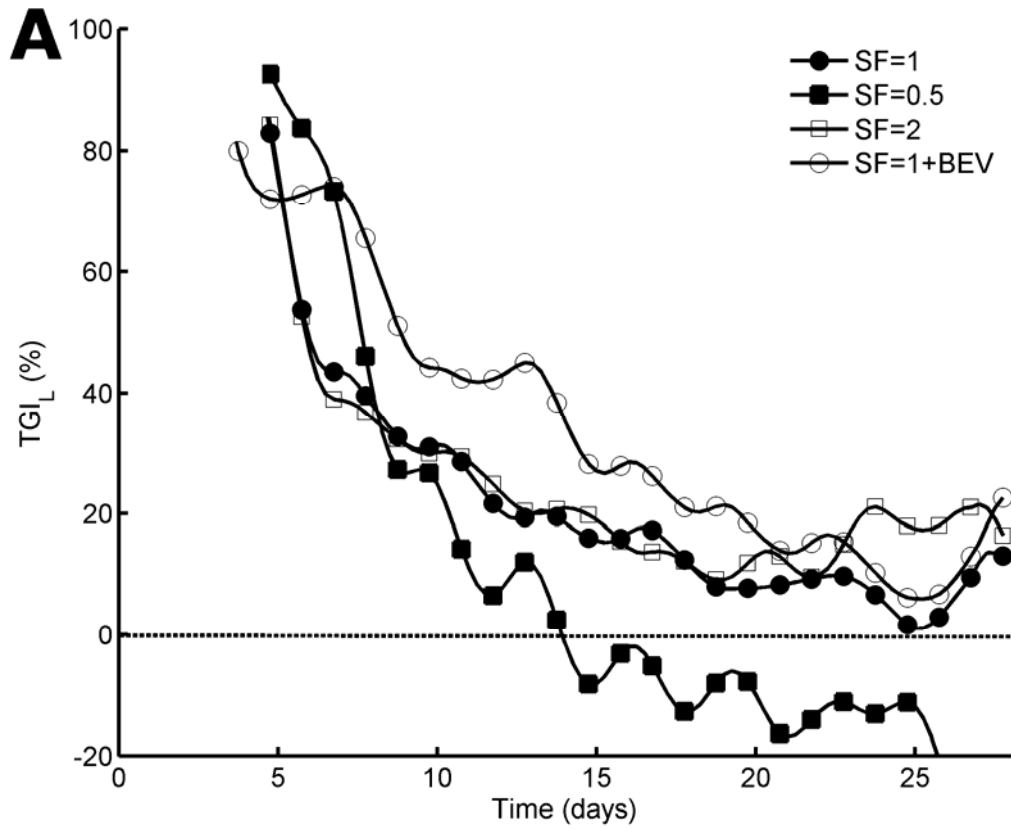


**Figure 3.** Model simulations of tumor dynamics in a patient after a single DOC dose (75 mg/m<sup>2</sup>, 1 hour IV infusion). A, Smoothed estimated TGI<sub>L</sub> after a single DOC dosing for tumors with different levels of angiogenesis intensity. Angiogenesis intensity is determined by scaling the model parameter, which combines VEGF secretion and activity rates. Simulations using two scaling factors (SF's), are compared to those with estimated angiogenesis intensity of the MCS patient (=1) and in combination with BEV (15mg/kg IV) are presented. Tumor dynamics were smoothed using a moving average algorithm with a span of 9 days. B, Predicted decrease in TGI<sub>L</sub> from day 7 to day 21 following DOC administration, as a function of angiogenesis intensity, relative to efficacy at 7 day intervals.

As mentioned above, a cytotoxic agent triggers a cascade of tumor recovery events. One would expect that tumor vascularization plays an important role in these processes. Our hypothesis was that increased effective vessel density correlates with faster recovery of the tumor from the chemotherapy induced damage (Gorelik et al., 2008a). Out of the many parameters that govern angiogenesis in the *in silico* model, the one that is responsible for vessel endothelial growth factor (VEGF) (Benjamin et al., 1999; Dor et al., 2001; Feng et al., 2007; Shweiki et al., 1992) secretion was chosen for the subsequent screening. The role of this growth factor in angiogenesis processes and its representation inside the computational model were discussed earlier in this chapter.

If the human MCS model is simulated with the VEGF secretion rate reduced by the factor of two compared to its original value, the predicted decrease in TGI<sub>L</sub> from day 7 to day 21 is only 29% (39% and 10%, respectively), indicating slower recovery from drug-induced tumor inhibition. In contrast, if the rate of new vessel formation is doubled compared to that calculated for the real MCS patient, the difference in the extent of tumor inhibition by DOC dose between day 7 and day 21 increases to 92%: 69% at day 7 vs. a negative value of -22% in day 21 (Fig. 3). This predicted growth of the tumor beyond that predicted for the untreated model is due to the extensive and rapid formation of blood vessels triggered by the chemotherapy. The impact of inter-dosing interval on the treatment efficacy is further amplified by the addition of bevacizumab (BEV) – an anti-angiogenic drug that binds the VEGF receptor, thus inhibiting its activity. The simulations of DOC/BEV administration to the original MCS model shows that initially

the tumor recovery is slow, with a predicted  $TGI_L$  value of 76% at day 7 compared to 45% without BEV. As time goes on, BEV is eliminated, which allows rapid angiogenesis and tumor recovery resulting in 10%  $TGI_L$  on day 21 (a difference of 66%).

These results suggest that if the MCS patient had less intensive angiogenesis, less frequent (for example tri-weekly) regimens would have been approximately as efficacious as once weekly, thus providing the clinicians more treatment alternatives. On the other hand, had the patient exhibited more intensive angiogenesis, the weekly DOC schedules would have been the only option to control the tumor growth, even at the cost of intolerable toxicity. Note, though, that our previous results in myelotoxicity modeling show that weekly DOC regimens are generally less toxic than the three-weekly ones [Vainas et al., 2008]. Fig. 3 demonstrates that the dependence of tumor recovery rate on the rate of angiogenesis is almost monotonic over a wide range of kinetic rates, which supports the generality of the above conclusions.

#### **4.4. Clinical relevance of the *in-silico* predictions**

The *in-silico* model presented here is composed of a large set of relatively simple mathematical equations that result in a highly complex predictive tool. The model parameters were estimated by comparison to a single patient suffering from a rare malignant condition – MCS. The impact of one angiogenesis-related model parameter (VEGF secretion rate) out of the many alternatives was tested, as explained in section 4.3 above. Nevertheless, the general principle of selecting inter-dose interval based on the angiogenesis status stems out of the mechanisms underlying the tumor dynamics. Thus, this hypothesis is not limited to any specific case, but is also expected for other cytotoxic agents and other solid tumors. Once this hypothesis is further validated, clinicians can use the angiogenesis status of their oncologic patients as an aid in personalization of cytotoxic treatment.

## **5. Use of angiogenesis models in drug salvage: the Virtual Patient technology**

Drug development is a challenging, costly and time consuming process. Drugs that fail in clinical trials often due to low efficacy and/or high toxicity levels are shelved or altogether discontinued (Lievre et al., 2001b). Since the pipelines of new compounds seem to be increasingly exhausted it becomes mandatory for pharmaceutical companies to revisit their decision-making process at all stages of drug development.

A new method is proposed here for salvaging prematurely shelved, or discontinued, compounds, whereby virtual clinical trials can be efficiently, accurately and rapidly carried out to test alternative treatment schedules or alternative patient populations for the discontinued drug. This can be done by computer simulations of synthetic patient populations, which allow for the drug-patient dynamic interactions and the characteristic distribution of numerous biological and drug response parameters in the real-life population. To illustrate this approach, we briefly discuss below a case study of a licensed drug, Sunitinib Malate (Sutent®, Pfizer Inc), in combination with a discontinued drug, ISIS-5132 (ISIS pharmaceuticals Inc), for the treatment of prostate cancer. Results based on the Virtual Patient technology suggest that a new combination treatment is predicted to result in more patients reaching a Progression Free Survival (PFS) at 5 years than with either Sunitinib Malate or ISIS-5132 monotherapy.

Each Virtual Patient in the synthetic population is constructed using a new bio-simulation technology developed to predict drug-patient dynamic interactions. It is based on the integration of the pharmacokinetics (PK) and pharmacodynamics (PD) of the drug or drugs in question with the bio-mathematical models of the pathological and the related physiological processes into one general framework (Arakelyan et al., 2005; Arakelyan et al., 2002). This method allows the prediction, not only of the short-term efficacy and toxicity effects of drugs, as conventional PK/PD models do, but also their long-term effects.

## 5.1. Constructing the disease model

The angiogenesis-dependant tumor model represents tumor growth and vessel dynamics (formation and maturation). The virtual tumor dynamics are affected by the values of its biological characteristics specified as model parameters. Since measurements of untreated cancer patients are not available, synthetic curves, mimicking the growth of untreated tumors may be constructed. These curves are based on initial tumor size measurements and doubling times of untreated cancer patients found in the literature (Feng et al., 2007; Lievre et al., 2001a; Usuda et al., 1994). Accordingly the size of the untreated tumor at a given moment can then be calculated using the exponential growth model as described by Usuda et al (Usuda et al., 1994).

Briefly, the following formula calculates the size of an untreated tumor on day  $t$ :

$$V_t = V_0 * 2^{t/VDT}$$

where  $t$  represents the time of measurement (in days),  $V_0$  represents the initial tumor size (in number of cells) and  $VDT$  represents the tumor volume doubling time. The synthetic curves that are generated by this process serve as an input for estimating the virtual cancer patients' average vascular tumor parameters ( $\vec{P}_{ave}$ ).

## 5.2. Constructing Synthetic Human Populations

In order to predict the effect of a treatment on a population, a virtual patient population must be generated. For each virtual patient the values of the model parameters are set. The individuals belonging to this population share most of the model parameters. However, several parameters are individually selected from a predefined distribution. The parameters and their values are selected based on studies indicating that they may have a prognostic value, and given that most of them are readily measured in the lab (Assikis et al., 2004; Caine et al., 2007; Maruyama et al., 2006).

### **5.3. Pharmacokinetics and Pharmacodynamics**

For the drugs analyzed here, PK profiles were modeled based on the literature information, suggesting a linear compartmental model based on the concentrations of the drugs in the plasma (Bello et al., 2006; Britten et al., 2008; O'Farrell et al., 2003; Stevenson et al., 1999; Tolcher et al., 2002). In addition, PD models for both drugs were estimated based on in-vitro and in-vivo data (Geiger et al., 1997; Mendel et al., 2003; Monia et al., 1996a; Monia et al., 1996b). The PK/PD effects were then allometrically scaled to human PK/PD (Administration, 2005; Contrera et al., 2004; FDA, 2005). A combined PK/PD model was created assuming an additive PD relationship with no PK interaction between the two drugs.

### **5.4. Drug salvage case study – combining chemotherapeutic and antiangiogenic drugs**

The compound ISIS-5132 (ISIS Pharmaceuticals, Inc.) is an antisense oligonucleotide targeted against the c-raf-1 kinase oncogene (Monia et al., 1996b; Monteith et al., 1998). The c-raf-1 kinase is the direct downstream mediator of the Ras protein whose oncogene version is associated with more than 30% of human solid tumor types including lung, colon, and pancreas cancers (Bos, 1989). ISIS-5132 has been tested in phase I trials in melanoma, pancreas, colorectal, breast, brain, small cell lung and non-small cell lung cancers (Cunningham et al., 2000; Rudin et al., 2001). Phase II studies were conducted in ovarian, prostate small cell lung and non-small cell lung cancers (Coudert et al., 2001; Cripps et al., 2002; Oza et al., 2003; Tolcher et al., 2002). However, these phase II trials failed to show significant antitumor activity. The compound has also been preclinically tested in xenograft models of breast, small cell lung, non-small cell lung, prostate, and colorectal cancer (Geiger et al., 1997). Prostate cancer was selected for this investigation given the availability of pre-clinical pharmacological data. We then ran virtual clinical trials for the ISIS-5132 compound as briefly described below.

The aim of this *in silico* study was to salvage ISIS-5132 for the treatment of prostate cancer by selecting a suitable drug on the market to use in combination with the ISIS

drug. This was done by performing virtual “Phase II” clinical trials in a synthetic prostate cancer patient population. In the first stage of this study many drug candidates were screened and analyzed (results not shown). Here we present the virtual clinical trial results of the combination of ISIS-5132 and Sunitinib Malate. Sunitinib Malate is a drug approved by the U.S. Food and Drug Administration (FDA) for advanced renal cell carcinoma (RCC) and gastrointestinal stromal cancer (GIST).

Model parameter, including drug PK and PD parameters, were based on experimental data reported in the literature. This parameter estimation process was performed separately for each of the drugs alone, and for the combination of the drugs. A concentration-effect function was created to assess the effect of ISIS-5132 on tumor cell proliferation. Similarly the effects of Sunitinib Malate on tumor cell proliferation on the number of pericytes and on the formation of new vessels were estimated based on the known drug mechanisms of action.

A synthetic human population was created and simulated under numerous possible regimens of Sunitinib/ISIS-5132 combinations (Table 1). Each of these simulated regimens was evaluated in terms of progression-free survival (PFS). Since the doubling time for untreated prostate cancer is one year and above (Egawa et al., 1997), we examined the efficacy of the studied drug combinations two and five years post treatment initiation.

**Table 1:** *Regimens simulated for ISIS-5132 and Sunitinib Malate*

Drug name	Route of administration	Dose*	Regimen**
Sunitinib malate	P.O.	25/37.5/ 50m $\xi$	1 week on 1 week off
	Every day (QD)		4 weeks on 2 weeks off
ISIS-5132	2 hours IV infusion Every 3 days (Q3D)	2-10 mg/kg	Every 3 days (Q3D)



*\* All combinations were administered both simultaneously and intermittently (Sunitinib Malate administered 1 week before ISIS-5132 and ISIS-5132 administered 1 week before Sunitinib Malate)*

*\*\* The duration of treatments was ca. 6 months*

The results are presented using Kaplan Meier Curve (KMC) survival analysis, which describes the probability of PFS at a given moment post- treatment (Fig. 4). For the purpose of this study, tumor progression is defined as an increase by a factor of 1.75 from the baseline tumor volume.

The simulations (Figs. 4, 5) predict more than 70% PFS of 5 years under the best selected regimen, under the accepted DLT, for the patient population, as compared to 40% in patients treated with Sunitinib Malate alone, and to 25% in ISIS-5132. The most effective regimen is ISIS-5132 6mg/kg Q3D + Sunitinib Malate 50mg, 4 weeks on – 2 weeks off. Note that the putative toxic effects of the studied combination were neglected in the current study for simplifying the demonstration. Exclusion of toxic effects may explain the visibly overestimated PFS. However, even if slightly over-estimated, these results clearly demonstrate the relative improvement of the ISIS-5132/Sunitinib Malate combination, thus providing an opportunity to salvage ISIS-5132 when administered in combination with Sunitinib Malate to prostate cancer patients.

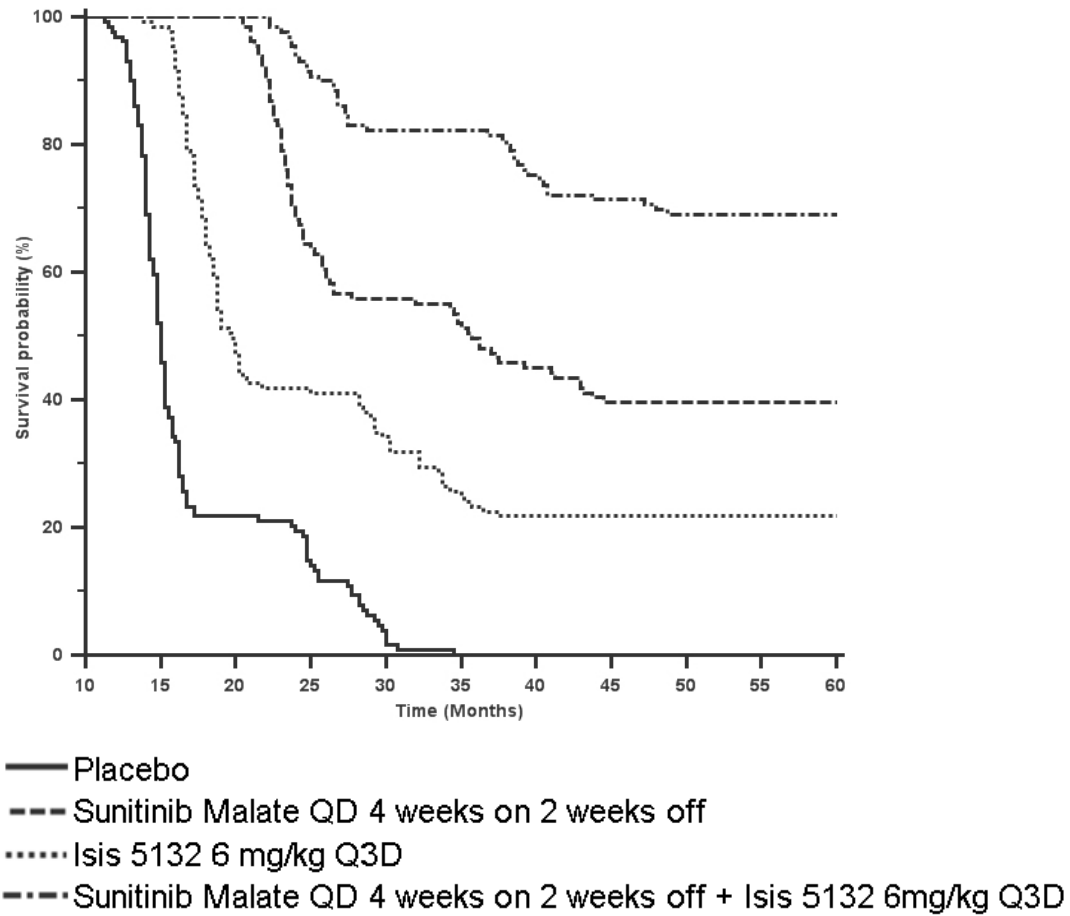
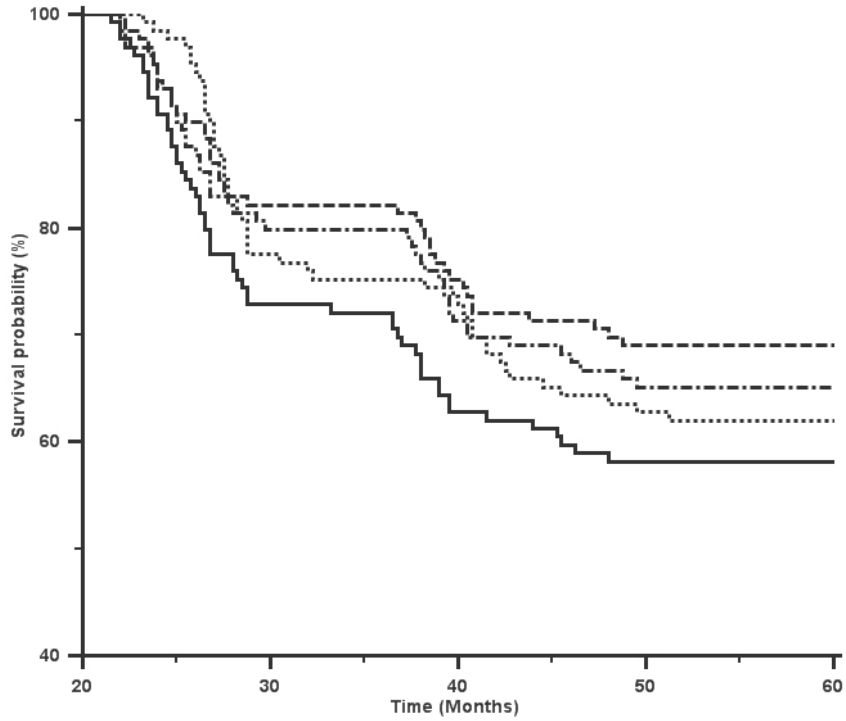


**Figure 4:** Simulation results of Progression Free Survival in a Synthetic Prostate Cancer Population under ISIS-5132 monotherapy, Sunitinib Malate monotherapy, and their combination (ISIS-5132 6mg/kg Q3D + Sunitinib Malate 50mg, 4 weeks on – 2 weeks off). Simulation results for an untreated Synthetic Prostate Cancer Populations are provided for comparison.



- Isis 5132 2mg/kg Q3D + Sunitinib Malate 50mg QD 4 weeks on 2 weeks off
- - - Isis 5132 6mg/kg Q3D + Sunitinib Malate 50mg QD 4 weeks on 2 weeks off
- ..... Isis 5132 6mg/kg Q3D + Sunitinib Malate 25mg QD 4 weeks on 2 weeks off
- · - Isis 5132 6mg/kg Q3D + Sunitinib Malate 37.5mg QD 4 weeks on 2 weeks off

**Figure 5:** Simulation results of Progression Free Survival in a Synthetic Prostate Cancer Populations under different schedules of ISIS-5132 and Sunitinib Malate combination therapy.

## 6. Summary and Conclusions

In this chapter we have illustrated how to construct mathematical models for angiogenesis at different levels of biological detail and at different levels of system complexity. We have shown that a more accurate, detailed and practical description of system dynamics can be obtained with a more complex model which accounts for more relevant components and processes. Even more importantly, mathematical modeling allows one to determine the minimal necessary components required to reproduce the observed phenomena and to understand how complex behavior emerges from basic system properties. Uncovered by rigorous mathematical analysis, fixed points and their stability can aid drug development, for example by supporting “go-no go” decisions in the early stages of target validation and drug discovery.

We described a new method for personalization of solid cancer pharmacotherapy. The method is based on mathematical models for angiogenesis embedded in the *in silico* Virtual Patient technology used in conjunction with data from tumor xenografts. We described a test case using this technology to suggest an improved treatment schedule for a particular MCS patient. An average accuracy of 87.1% was obtained when comparing *in silico* model predictions to the observed tumor growth inhibition in the xenografted animals. Model predictions suggested that a regimen containing Bevacizumab applied intravenously in combination with once-weekly Docetaxel is more efficacious in the MCS patient compared to other simulated schedules. Weekly Docetaxel in the patient resulted in stable metastatic disease and relief of pancytopenia due to tumor infiltration. Based on numerical investigation of the model, we suggest that the advantage of weekly Docetaxel versus the tri-weekly regimen is directly related to the tumor's angiogenesis intensity.

Finally, we described a new method for salvaging prematurely shelved, or discontinued, drugs. Virtual clinical trials were efficiently, accurately and rapidly simulated to test alternative treatment schedules, for the discontinued drug. We illustrated this approach by discussing a case study of a licensed drug, Sunitinib Malate (Sutent®, Pfizer Inc), in

combination with a discontinued drug, ISIS-5132 (ISIS pharmaceuticals Inc), for the treatment of prostate cancer. Results based on the Virtual Patient technology suggest that a novel combination treatment is predicted to result in more patients reaching Progression Free Survival (PFS) at 5 years compared to either Sunitinib Malate or ISIS-5132 monotherapy.

## References

- Agur, Z. (1986). The effect of drug schedule on responsiveness to chemotherapy. *Annals NY Acad Sci*, 274-277.
- Agur, Z. (1998). Resonance and anti-resonance in the design of chemotherapeutic protocols. *J Theor Med I*, 237-245.
- Agur, Z., Arakelyan, L., Daugulis, P., and Ginosar, Y. (2004). Hopf point analysis for angiogenesis models. *Disc Cont Dyn Systems 4*, 29-38.
- Agur, Z., Arnon, R., and Schechter, B. (1988). Reduction of cytotoxicity to normal tissues by new regimens of cell-cycle phase-specific drugs. *Mathematical Biosciences* 92, 1-15.
- Agur, Z., Arnon, R., and Schechter, B. (1992). Effect of the dosing interval on myelotoxicity and survival in mice treated by cytarabine. *Eur J Cancer* 28A, 1085-1090.
- Agur, Z., Kogan, Y., Kheiffetz, Y., Ziv, I., Shoham, M., and Vainstein, V. (2008). Mathematical modeling as a new approach for improving the efficacy/toxicity profile of drugs: the thrombocytopenia case study (John Wiley & Sons, USA).
- Alarcon, T., Byrne, H., Maini, P., and Panovska, J. (2006 ). Mathematical modelling of angiogenesis and vascular adaptation, in: *Studies in Multidisciplinarity, Vol 3* (Elsevier B.V.).
- Arakelyan, L., Daugulis, P., Ginosar, Y., Vainstein, V., Selister, V., Kogan, Y., Harpak, H., and Agur, Z. (2003a). Multi-scale analysis of angiogenic dynamics and therapy, Vol Vol. Ch. 7. (CRC Press, LLC, (UK).).
- Arakelyan, L., Daugulis, P., Ginosar, Y., Vainstein, V., Selister, V., Kogan, Y., Harpak, H., and Agur, Z. (2003b). Multi-scale analysis of angiogenic dynamics and therapy. In *Cancer Modelling and Simulation*, L. Preziosi, ed. (CRC Press, LLC, (UK).).
- Arakelyan, L., Merbl, Y., and Agur, Z. (2005). Vessel maturation effects on tumour growth: validation of a computer model in implanted human ovarian carcinoma spheroids. *Eur J Cancer* 41, 159-167.
- Arakelyan, L., Vainstein, V., and Agur, Z. (2002). A computer algorithm describing the process of vessel formation and maturation, and its use for predicting the effects of anti-angiogenic and anti-maturation therapy on vascular tumor growth. *Angiogenesis* 5, 203-214.
- Araujo, R.P., and McElwain, D.L. (2004). A history of the study of solid tumour growth: the contribution of mathematical modelling. *Bull Math Biol* 66, 1039-1091.
- Assikis, V.J., Do, K.A., Wen, S., Wang, X., Cho-Vega, J.H., Brisbay, S., Lopez, R., Logothetis, C.J., Troncoso, P., Papandreou, C.N., *et al.* (2004). Clinical and biomarker correlates of androgen-independent, locally aggressive prostate cancer with limited metastatic potential. *Clin Cancer Res* 10, 6770-6778.
- Bello, C.L., Sherman, L., Zhou, J., Verkh, L., Smeraglia, J., Mount, J., and Klamerus, K.J. (2006). Effect of food on the pharmacokinetics of sunitinib malate (SU11248), a multi-targeted receptor tyrosine kinase inhibitor: results from a phase I study in healthy subjects. *Anticancer Drugs* 17, 353-358.

- Benjamin, L.E., Golijanin, D., Itin, A., Pode, D., and Keshet, E. (1999). Selective ablation of immature blood vessels in established human tumors follows vascular endothelial growth factor withdrawal. *J Clin Invest* *103*, 159-165.
- Bergers, G., Song, S., Meyer-Morse, N., Bergsland, E., and Hanahan, D. (2003). Benefits of targeting both pericytes and endothelial cells in the tumor vasculature with kinase inhibitors. *J Clin Invest* *111*, 1287-1295.
- Bodnar, M., and Forys, U. Angiogenesis model with carrying capacity depending on vessel density.
- Bos, J.L. (1989). ras oncogenes in human cancer: a review. *Cancer Res* *49*, 4682-4689.
- Britten, C.D., Kabbinar, F., Hecht, J.R., Bello, C.L., Li, J., Baum, C., and Slamon, D. (2008). A phase I and pharmacokinetic study of sunitinib administered daily for 2 weeks, followed by a 1-week off period. *Cancer Chemother Pharmacol* *61*, 515-524.
- Byrne, H.M. (1999). A weakly nonlinear analysis of a model of avascular solid tumour growth. *J Math Biol* *39*, 59-89.
- Caine, G.J., Ryan, P., Lip, G.Y., and Blann, A.D. (2007). Significant decrease in angiopoietin-1 and angiopoietin-2 after radical prostatectomy in prostate cancer patients. *Cancer Lett* *251*, 296-301.
- Chao, K.S. (2007). 3'-deoxy-3'-(18)F-fluorothymidine (FLT) positron emission tomography for early prediction of response to chemoradiotherapy--a clinical application model of esophageal cancer. *Semin Oncol* *34*, S31-36.
- Chen, J.P., Lo, Y., Yu, C.J., Hsu, C., Shih, J.Y., and Yang, C.H. (2008). Predictors of toxicity of weekly docetaxel in chemotherapy-treated non-small cell lung cancers. *Lung Cancer* *60*, 92-97.
- Contrera, J.F., Matthews, E.J., Kruhlak, N.L., and Benz, R.D. (2004). Estimating the safe starting dose in phase I clinical trials and no observed effect level based on QSAR modeling of the human maximum recommended daily dose. *Regul Toxicol Pharmacol* *40*, 185-206.
- Coudert, B., Anthony, A., Fiedler, W., Droz, J.P., Dieras, V., Borner, M., Smyth, J.F., Morant, R., de Vries, M.J., Roelvink, M., *et al.* (2001). Phase II trial with ISIS 5132 in patients with small-cell (SCLC) and non-small cell (NSCLC) lung cancer. A European Organization for Research and Treatment of Cancer (EORTC) Early Clinical Studies Group report. *Eur J Cancer* *37*, 2194-2198.
- Cripps, M.C., Figueredo, A.T., Oza, A.M., Taylor, M.J., Fields, A.L., Holmlund, J.T., McIntosh, L.W., Geary, R.S., and Eisenhauer, E.A. (2002). Phase II randomized study of ISIS 3521 and ISIS 5132 in patients with locally advanced or metastatic colorectal cancer: a National Cancer Institute of Canada clinical trials group study. *Clin Cancer Res* *8*, 2188-2192.
- Cunningham, C.C., Holmlund, J.T., Schiller, J.H., Geary, R.S., Kwoh, T.J., Dorr, A., and Nemunaitis, J. (2000). A phase I trial of c-Raf kinase antisense oligonucleotide ISIS 5132 administered as a continuous intravenous infusion in patients with advanced cancer. *Clin Cancer Res* *6*, 1626-1631.
- Deakin, A.S. (1976). Model for initial vascular patterns in melanoma transplants. *Growth* *40*, 191-201.

- Dor, Y., Porat, R., and Keshet, E. (2001). Vascular endothelial growth factor and vascular adjustments to perturbations in oxygen homeostasis. *Am J Physiol Cell Physiol* 280, C1367-1374.
- Egawa, S., Matsumoto, K., Iwamura, M., Uchida, T., Kuwao, S., and Koshiba, K. (1997). Impact of life expectancy and tumor doubling time on the clinical significance of prostate cancer in Japan. *Jpn J Clin Oncol* 27, 394-400.
- Fatima, S.F., Kaya, A., Visser, T.T.P., Hartong, S.C.C., Agur, Z., and Wagemaker, G. (2008). Efficacy of recombinant human and rhesus thrombopoietin stimulated blood transfusions in comparison to unstimulated whole blood or thrombocyte transfusions in a non-human primate model. In (European Hematology Association (EHA) 13th Congress, Copenhagen, Denmark).
- FDA (2005). Guidance for Industry Estimating the Maximum Safe Starting Dose in Initial Clinical Trials for Therapeutics in Adult Healthy Volunteers. In Services, USDoHaH and FaD Administration (Food and Drug Administration Center for Drug Evaluation and Research (CDER) ).
- Feng, Y., vom Hagen, F., Pfister, F., Djokic, S., Hoffmann, S., Back, W., Wagner, P., Lin, J., Deutsch, U., and Hammes, H.P. (2007). Impaired pericyte recruitment and abnormal retinal angiogenesis as a result of angiopoietin-2 overexpression. *Thromb Haemost* 97, 99-108.
- Folkman, J. (1971). Tumor angiogenesis: therapeutic implications. *N Engl J Med* 285, 1182-1186.
- Forys, U., Kheifetz, Y., and Kogan, Y. (2005). Critical-point analysis for three-variable cancer angiogenesis modeling. *Math Biosci and Eng* 2 511-525.
- Freyer, J.P., and Sutherland, R.M. (1980). Selective dissociation and characterization of cells from different regions of multicell tumor spheroids. *Cancer Res* 40, 3956-3965.
- Geiger, T., Muller, M., Monia, B.P., and Fabbro, D. (1997). Antitumor activity of a C-raf antisense oligonucleotide in combination with standard chemotherapeutic agents against various human tumors transplanted subcutaneously into nude mice. *Clin Cancer Res* 3, 1179-1185.
- Gilead, A., Meir, G., and Neeman, M. (2004). The role of angiogenesis, vascular maturation, regression and stroma infiltration in dormancy and growth of implanted MLS ovarian carcinoma spheroids. *Int J Cancer* 108, 524-531.
- Gilead, A., and Neeman, M. (1999). Dynamic remodeling of the vascular bed precedes tumor growth: MLS ovarian carcinoma spheroids implanted in nude mice. *Neoplasia* 1, 226-230.
- Gorelik, B., Ziv, I., Shohat, R., Wick, M., Hankins, D., Sidransky, D., and Agur, Z. (2008a). Efficacy of Weekly Docetaxel and Bevacizumab in Mesenchymal Chondrosarcoma: a New Theranostic Method combining Xenografted Biopsies with a Mathematical Model. . *Cancer Research*
- Gorelik, B., Ziv, I., Shohat, R., Wick, M., Hankins, W.D., Sidransky, D., and Agur, Z. (2008b). Efficacy of weekly docetaxel and bevacizumab in mesenchymal chondrosarcoma: a new theranostic method combining xenografted biopsies with a mathematical model. *Cancer Res* 68, 9033-9040.
- Greenspan, H.P. (1974). On the self-inhibited growth of cell cultures. *Growth* 38, 81-95.



- Hahnfeldt, P., Panigrahy, D., Folkman, J., and Hlatky, L. (1999). Tumor development under angiogenic signaling: a dynamical theory of tumor growth, treatment response, and postvascular dormancy. *Cancer Res* 59, 4770-4775.
- Holash, J., Wiegand, S.J., and Yancopoulos, G.D. (1999). New model of tumor angiogenesis: dynamic balance between vessel regression and growth mediated by angiopoietins and VEGF. *Oncogene* 18, 5356-5362.
- Iwao-Koizumi, K., Matoba, R., Ueno, N., Kim, S.J., Ando, A., Miyoshi, Y., Maeda, E., Noguchi, S., and Kato, K. (2005). Prediction of docetaxel response in human breast cancer by gene expression profiling. *J Clin Oncol* 23, 422-431.
- Karam, J.A., Svatek, R.S., Karakiewicz, P.I., Gallina, A., Roehrborn, C.G., Slawin, K.M., and Shariat, S.F. (2008). Use of preoperative plasma endoglin for prediction of lymph node metastasis in patients with clinically localized prostate cancer. *Clin Cancer Res* 14, 1418-1422.
- Kimura, Y., Sumi, M., Sakihama, N., Tanaka, F., Takahashi, H., and Nakamura, T. (2008). MR Imaging Criteria for the Prediction of Extranodal Spread of Metastatic Cancer in the Neck. *AJNR Am J Neuroradiol*.
- Kunz-Schughart, L.A. (1999). Multicellular tumor spheroids: intermediates between monolayer culture and in vivo tumor. *Cell Biol Int* 23, 157-161.
- Landry, J., Freyer, J.P., and Sutherland, R.M. (1982). A model for the growth of multicellular spheroids. *Cell Tissue Kinet* 15, 585-594.
- Lievre, M., Menard, J., Bruckert, E., Cogneau, J., Delahaye, F., Giral, P., Leitersdorf, E., Luc, G., Masana, L., Moulin, P., *et al.* (2001a). Premature discontinuation of clinical trial for reasons not related to efficacy, safety, or feasibility. *British Medical Journal* 322, 603-605.
- Liotta, L.A., Saidel, G.M., and Kleinerman, J. (1977). Diffusion model of tumor vascularization and growth. *Bull Math Biol* 39, 117-128.
- Mantzaris, N.V., Webb, S., and Othmer, H.G. (2004). Mathematical modeling of tumor-induced angiogenesis. *J Math Biol* 49, 111-187.
- Marusić, M., Bajzer, Z., Vuk-Pavlović, S., and JP., F. (1994). Tumor growth in vivo and as multicellular spheroids compared by mathematical models. *Bull Math Biol* 56, 617-631.
- Maruyama, Y., Ono, M., Kawahara, A., Yokoyama, T., Basaki, Y., Kage, M., Aoyagi, S., Kinoshita, H., and Kuwano, M. (2006). Tumor growth suppression in pancreatic cancer by a putative metastasis suppressor gene Cap43/NDRG1/Drg-1 through modulation of angiogenesis. *Cancer Res* 66, 6233-6242.
- Matthews, B.W. (2007). Protein Structure Initiative: getting into gear. *Nat Struct Mol Biol* 14, 459-460.
- McLeod, H.L. (2002). Individualized cancer therapy: molecular approaches to the prediction of tumor response. *Expert Rev Anticancer Ther* 2, 113-119.
- Mendel, D.B., Laird, A.D., Xin, X., Louie, S.G., Christensen, J.G., Li, G., Schreck, R.E., Abrams, T.J., Ngai, T.J., Lee, L.B., *et al.* (2003). In vivo antitumor activity of SU11248, a novel tyrosine kinase inhibitor targeting vascular endothelial growth factor and platelet-derived growth factor receptors: determination of a pharmacokinetic/pharmacodynamic relationship. *Clin Cancer Res* 9, 327-337.

- Monia, B.P., Johnston, J.F., Geiger, T., Muller, M., and Fabbro, D. (1996a). Antitumor activity of a phosphorothioate antisense oligodeoxynucleotide targeted against C-raf kinase. *Nat Med* 2, 668-675.
- Monia, B.P., Sasmor, H., Johnston, J.F., Freier, S.M., Lesnik, E.A., Muller, M., Geiger, T., Altmann, K.H., Moser, H., and Fabbro, D. (1996b). Sequence-specific antitumor activity of a phosphorothioate oligodeoxyribonucleotide targeted to human C-raf kinase supports an antisense mechanism of action in vivo. *Proc Natl Acad Sci U S A* 93, 15481-15484.
- Monteith, D.K., Geary, R.S., Leeds, J.M., Johnston, J., Monia, B.P., and Levin, A.A. (1998). Preclinical evaluation of the effects of a novel antisense compound targeting C-raf kinase in mice and monkeys. *Toxicol Sci* 46, 365-375.
- O'Farrell, A.M., Foran, J.M., Fiedler, W., Serve, H., Paquette, R.L., Cooper, M.A., Yuen, H.A., Louie, S.G., Kim, H., Nicholas, S., *et al.* (2003). An innovative phase I clinical study demonstrates inhibition of FLT3 phosphorylation by SU11248 in acute myeloid leukemia patients. *Clin Cancer Res* 9, 5465-5476.
- Oza, A.M., Elit, L., Swenerton, K., Faught, W., Ghatage, P., Carey, M., McIntosh, L., Dorr, A., Holmlund, J.T., and Eisenhauer, E. (2003). Phase II study of CGP 69846A (ISIS 5132) in recurrent epithelial ovarian cancer: an NCIC clinical trials group study (NCIC IND.116). *Gynecol Oncol* 89, 129-133.
- Quesada, A.R., Medina, M.A., and Alba, E. (2007). Playing only one instrument may be not enough: limitations and future of the antiangiogenic treatment of cancer. *Bioessays* 29, 1159-1168.
- Rudin, C.M., Holmlund, J., Fleming, G.F., Mani, S., Stadler, W.M., Schumm, P., Monia, B.P., Johnston, J.F., Geary, R., Yu, R.Z., *et al.* (2001). Phase I Trial of ISIS 5132, an antisense oligonucleotide inhibitor of c-raf-1, administered by 24-hour weekly infusion to patients with advanced cancer. *Clin Cancer Res* 7, 1214-1220.
- Sachs, R., Hlatky, L., and Hahnfeldt, P. (2001). Simple ODE models of tumor growth and anti-angiogenic or radiation treatment. *Mathematical and Computer Modelling* 33, 1297-1305.
- Saidel, G.M., Liotta, L.A., and Kleinerman, J. (1976). System dynamics of metastatic process from an implanted tumor. *J Theor Biol* 56, 417-434.
- Salter, K.H., Acharya, C.R., Walters, K.S., Redman, R., Anguiano, A., Garman, K.S., Anders, C.K., Mukherjee, S., Dressman, H.K., Barry, W.T., *et al.* (2008). An integrated approach to the prediction of chemotherapeutic response in patients with breast cancer. *PLoS ONE* 3, e1908.
- Segel, L.A., ed. (1984). *Modeling Dynamic Phenomena in Molecular and Cellular Biology* (Cambridge University Press).
- Shweiki, D., Itin, A., Soffer, D., and Keshet, E. (1992). Vascular endothelial growth factor induced by hypoxia may mediate hypoxia-initiated angiogenesis. *Nature* 359, 843-845.
- Skehan, P. (1986). On the normality of growth dynamics of neoplasms in vivo: a data base analysis. *Growth* 50, 496-515.
- Skomorovski, K., Harpak, H., Ianovski, A., Vardi, M., Visser, T.P., Hartong, S.C., van Vliet, H.H., Wagemaker, G., and Agur, Z. (2003). New TPO treatment schedules of increased safety and efficacy: pre-clinical validation of a thrombopoiesis simulation model. *Br J Haematol* 123, 683-691.

- Spratt, J.S., Meyer, J.S., and Spratt, J.A. (1996). Rates of growth of human neoplasms: Part II. *J Surg Oncol* *61*, 68-83.
- Stevenson, J.P., Yao, K.S., Gallagher, M., Friedland, D., Mitchell, E.P., Cassella, A., Monia, B., Kwoh, T.J., Yu, R., Holmlund, J., *et al.* (1999). Phase I clinical/pharmacokinetic and pharmacodynamic trial of the c-raf-1 antisense oligonucleotide ISIS 5132 (CGP 69846A). *J Clin Oncol* *17*, 2227-2236.
- Sutherland, R.M., McCredie, J.A., and Inch, W.R. (1971). Growth of multicell spheroids in tissue culture as a model of nodular carcinomas. *J Natl Cancer Inst* *46*, 113-120.
- Tolcher, A.W., Reyno, L., Venner, P.M., Ernst, S.D., Moore, M., Geary, R.S., Chi, K., Hall, S., Walsh, W., Dorr, A., *et al.* (2002). A randomized phase II and pharmacokinetic study of the antisense oligonucleotides ISIS 3521 and ISIS 5132 in patients with hormone-refractory prostate cancer. *Clin Cancer Res* *8*, 2530-2535.
- Usuda, K., Saito, Y., Sagawa, M., Sato, M., Kanma, K., Takahashi, S., Endo, C., Chen, Y., Sakurada, A., and Fujimura, S. (1994). Tumor doubling time and prognostic assessment of patients with primary lung cancer. *Cancer* *74*, 2239-2244.
- Venter, J.C., Adams, M.D., Myers, E.W., Li, P.W., Mural, R.J., Sutton, G.G., Smith, H.O., Yandell, M., Evans, C.A., Holt, R.A., *et al.* (2001). The sequence of the human genome. *Science* *291*, 1304-1351.
- Walker, I., Newell, H. (2008). Do molecularly targeted agents in oncology have reduced attrition rates? *Nature Reviews Drug Discovery* *Vol.8* pp. 15-16.
- Warm, M., Nawroth, F., Ohlinger, R., Valter, M., Pantke, E., Mallmann, P., Harbeck, N., Kates, R., and Thomas, A. (2007). Improvement of safety profile of docetaxel by weekly administration in patients with metastatic breast cancer. *Onkologie* *30*, 436-441.
- Wieder, H.A., Geinitz, H., Rosenberg, R., Lordick, F., Becker, K., Stahl, A., Rummeny, E., Siewert, J.R., Schwaiger, M., and Stollfuss, J. (2007). PET imaging with [18F]3'-deoxy-3'-fluorothymidine for prediction of response to neoadjuvant treatment in patients with rectal cancer. *Eur J Nucl Med Mol Imaging* *34*, 878-883.
- Ziv, I., Shohat, R., Wick, M., Webb, C., Hankins, D., Sidransky, D., and Agur, Z. (2006). Novel Virtual Patient technology for predicting response of breast cancer and mesenchymal chondrosarcoma patients to mono- and combination therapy by cytotoxic and targeted drugs. . Paper presented at: AACR-NCI-EORTC--18th symposium: Molecular targets and cancer therapeutics (Prague Czech republic).